Elsevier Editorial System(tm) for Neurobiology of Disease

Manuscript Draft

Manuscript Number: NBD-16-655R1

Title: A Saposin deficiency model in Drosophila: lysosomal storage, progressive neurodegeneration and sensory physiological decline

Article Type: Research paper

Keywords: prosaposin, saposin, lysosomal storage disease, neurodegeneration, Drosophila

Corresponding Author: Dr. Sean Thomas Sweeney, PhD

Corresponding Author's Institution: University of York

First Author: Samantha Hindle

Order of Authors: Samantha Hindle; Sarita Hebbar; Dominik Schwudke; Christopher Elliott; Sean Thomas Sweeney, PhD

Abstract: Saposin deficiency is a childhood neurodegenerative lysosomal storage disorder (LSD) that can cause premature death within three months of life. Saposins are activator proteins that promote the function of lysosomal hydrolases that mediate the degradation of sphingolipids. There are four saposin proteins in humans, which are encoded by the prosaposin gene. Mutations causing an absence or impaired function of individual saposins or the whole prosaposin gene lead to distinct LSDs due to the storage of different classes of sphingolipids. The pathological events leading to neuronal dysfunction induced by lysosomal storage of sphingolipids are as yet poorly defined. We have generated and characterised a Drosophila model of saposin deficiency that shows striking similarities to the human diseases. Drosophila saposin-related (dSap-r) mutants show a reduced longevity, progressive neurodegeneration, lysosomal storage, dramatic swelling of neuronal soma, perturbations in sphingolipid catabolism, and sensory physiological deterioration. Our data suggests a genetic interaction with a calcium exchanger (Calx) pointing to a possible calcium homeostasis deficit in dSap-r mutants. Together these findings support the use of dSap-r mutants in advancing our understanding of the cellular pathology implicated in saposin deficiency and related LSDs.

Cover Letter

UNIVERSITY of York

DEPARTMENT OF BIOLOGY (AREA 9)
Wentworth Way, Heslington,
YORK YO10 5DD U. K.

Sean T. Sweeney, Ph.D.
Reader in Neuroscience,
Department of Biology
Direct Telephone: (01904) 328537
Direct Facsimile: (01904) 328505
email: sean.sweeney@york.ac.uk

To: Prof. Timothy Greenamyre
Editor-in-Chief
Neurobiology of Disease

Ms. No.: NBD-16-655
Title: A Saposin deficiency model in Drosophila: lysosomal storage, progressive neurodegeneration, sensory physiological decline and defective calcium homeostasis
Corresponding Author: Dr. Sean Thomas Sweeney
Authors: Samantha Hindle; Sarita Hebbar; Dominik Schwudke; Christopher Elliott;

Dear Professor Greenamyre

We would like to thank you and the two insightful reviewers for your consideration and very fair treatment of our manuscript. We have modified the manuscript in the light of the comments, particularly reviewer #3 who suggested some textual restructuring and reformatting of figures which we have completed. Reviewer #2 suggested omitting our data on the genetic interaction between our Sap-r mutants and expression of the CalX transporter. We have overall toned down our interpretation and conclusions from this experiment, but feel that the data we have generated here is still instructive to the physiological phenotype and understanding of the saposin-deficiency condition. We agree with nearly all the reviewers comments and a point by point reply is appended below. We have submitted a Word document with the edits still evident, in addition to our final version of the manuscript. We feel that these revisions have improved the manuscript and we hope that you will be in agreement.

I would like to bring to your notice that I was asked on 30th of September to review a submitted manuscript on a Drosophila model of saposin-deficiency by the Disease Models and Mechanisms journal. For reasons of 'conflict of interest' I declined to review the manuscript, but a perusal of the abstract suggests that much of our data is in concurrence.

In summary, we feel we have now delivered a study that covers a lot of new ground in the delivery of a novel model of Saposin-deficiency. We recapitulate the cellular and physiological hallmarks of the disease and pinpoint dysfunction in lipid homeostasis, in particular the increase in sphingosine, with a putative link to calcium dysregulation and a catastrophic loss in sensory function.

We would like to thank you for your care and interest in our manuscript and we look forward to hearing from you in the near future.

Yours sincerely

Sean Sweeney

Sean Sweeney PhD.

Responses to Reviewers

Reviewer #2: In their manuscript "A Saposin deficiency model in Drosophila: lysosomal storage, progressive neurodegeneration, sensory physiological decline and defective calcium homeostasis" the authors identify the drosophila saponin, demonstrate the saponin distribution in the nervous system using saponin reporter flies, and describe the phenotypes of saponin deficiency and overexpression. With saponin deficiency they find phenotypes reminiscent of human lysosomal storage diseases.

The manuscript is very well written. The rationale for investigating saponin in drosophila and the applied methods are clearly described. In the description of the lysosomal storage disorder in the mutant flies, the authors applied numerous advanced techniques including electron microscopy and mass spectrometry measurements of lipids.

We would like to thank the reviewer for their generous comments.

The model alone, however, does not provide new mechanistic insight, in particular since saponins appear expressed primarily in glial cells in flies, which does not mirror the human situation.
For the two areas of mechanistic insight, the authors do not provide sufficient data to support their conclusions (see major issues).

*We would differ with the reviewer in severity of their conclusion. We have, however, modified our comments to reflect the limitations of our data in the light of this comment. The expression of saposins in glia does not obviate a function for saposins in neurons. Prosaposins are pro-glycoproteins, that are trafficked through the secretory system to the lysosome, but are also simultaneously secreted from the cell. The majority of such proteins studied to date can be secreted from an expressing cell and taken up in a paracrine fashion by non-expressing cells via the Mannose-6-phosphate receptor-scavenging pathway to deliver protein to the lysosome of the non-expressing cell. Indeed, this mechanism is the cellular basis for 'replacement therapy' in many of the treatable lysosomal storage diseases. Our conclusion section on this data now reads: '*In addition, mammalian prosaposin is abundant in secretory fluids, including cerebrospinal fluid, seminal fluid, milk, bile and pancreatic fluid (48-51); in fact prosaposin is one of the main secretory products of Sertoli cells in the male reproductive system (52). Therefore, it is quite possible that *Drosophila* glia provide dSap-r to neurons by glial secretion and neuronal uptake. This notion is consistent with our findings that *dSap-r* mutant longevity can be substantially rescued by expressing *dSap-r* directly in neurons, which suggests a neuronal requirement for dSap-r. This potential non-autonomous function of dSap-r has important implications for future therapeutic strategies as it suggests that a source of prosaposin secreting cells could provide a successful intervention for these conditions.'**

Major issues:
- Neuronal vs glial saponin: Using reporter flies that express GFP from the

saponin promoter, the authors demonstrate that saponins are expressed in glial cells but not in neurons (Figure 1C). In contrast, the authors find that premature death in saponin-deficient flies can be rescued not only by expression of saponin from a glial promoter, but also from a neuronal promoter (Figure 2). The authors suggest that transfer of saponins from glia to neurons underlies this discrepancy, but provide no further data to support this hypothesis. In contrast to the advanced methods used in the first part of the manuscript, this part seems half-hearted. Even fairly simple experiments could provide further insight into this discrepancy and support or dismiss the authors' hypothesis: Does the distribution of saponin as assayed by immunocytochemistry differ from the distribution of GFP in the saponin reporter flies? Could the promoters used for neuronal vs glial expression of saponin be leaky? What are the consequences of neuronal vs. glial expression of saponin siRNA?

*We would dearly have liked to address this issue. To do so we made two separate antibodies to dSap-r, (a total of four rabbits sacrificed), but despite extensive testing, the anti-sera generated would not recognise any dSap-r proteins by immunocytochemistry and were limited in their detection of protein by western blot. This took a great deal of time and effort, so we feel our efforts were not 'half-hearted'. To support our promoter data, we cite the very clear in situ expression data from Marc Freeman for dSap-r that shows a very clear signal for glial expression, but none in the absence of 'glial cells missing' a glial expressed transcription factor in the late embryonic CNS of Drosophila (Figure 2, Freeman et al.,(2003)Neuron 38, 567-580). The promoter constructs used, 1407-GAL4 and repo-GAL4 are very well characterised and extensively used by the Drosophila community and are considered as 'clean' as any promoter construct can be. However, we temper our conclusions with the following wording and additional reference: '*Although mammalian saposins are expressed in neurons, our findings suggested that *dSap-r* is either not expressed in neurons or is expressed at a level below the threshold of our reporter. Transcriptomic data from FACS isolated neurons, glia and surface glia (blood-brain barrier) (74) shows that *dSap-r* is expressed in neurons, glia and surface glia, and may therefore be more ubiquitous than the *dSap-r*^{NP7456} GAL4 enhancer-trap is reporting.'*

Figure 5 does not support the transfer of saponin from glia to neurons since it is not unexpected to observe neuronal swelling in flies with a glial pathology.

We are of a difference of opinion here, we feel it would be unexpected for neurons to have a very clear lysosomal storage disorder phenotype, at the level of multi-lamellar inclusions, due to glial dysfunction only.

- The role of calcium: The already reduced ERG in saponin deficient flies is reduced further by overexpression of CalX. From this observation the authors conclude that calcium is low in saponin deficient flies. The data provided for this conclusion is not sufficient. The argument that the ERG is reduced further when another mutation is added to an already perturbed system is not convincing, in particular when the additional mutation is in a neuronal membrane protein related to ion transport. There are numerous well-

established techniques to report intracellular calcium, so it is not clear why the authors chose the very indirect approach with CalX.

*We agree that our approach may be indirect, but the physiological read-out is very functional and clear at the level of sensory function. Our strategy, given the tools immediately to hand, is to use genetics first, and follow up with other methods. Unfortunately we do not have the microscopical set-up readily to hand to image calcium fluxes in sensory neurons, so we have settled with our physiological and genetical analysis. We have however, toned down our interpretation and conclusions of the data as follows: '*This significant genetic interaction suggests that calcium regulation may be compromised in *dSap-r* mutant photoreceptors, leading to neurodegeneration and perturbed sensory function. Further work is required to determine the severity of the calcium homeostasis defect in *dSap-r* mutants, including its temporal and spatial (neurons vs glia) involvement.'

The authors may also choose to remove the CalX experiments and devote a second manuscript to the investigation of calcium in this fly model.

As above, we have now toned down our conclusions from the CalX experiments and in this light would prefer to include this data in the manuscript for we feel it is of interest to the field.

Minor issues:
- the term "dSap-r flies" used for saponin deficient flies throughout the manuscript is confusing. It woulbe be better to call them "dSap-r deficient flies". *Done*
- page 7: "MS measurements" should be spelled out. *Done*
- the effect of the Df mutant fly should be explained so that readers outside the drosophila field can follow. *Done*
- page 14: "Arl8 western analysis" is colloquial, add "blot". *Done*

Reviewer #3: The study reports the establishment of new Drosophila mutants that represent - to my knowledge - the first fly model of saposin deficiency. This is a highly welcome addition to the existing panel of animal models for lysosomal storage disorders. Its use will provide new insight into disease mechanisms and may help to develop new therapeutic strategies. A critical point is the thorough characterization of the model. The authors reveal that mutations in the Drosophila homologue of prosaposin cause shorten the life span, cause accumulation of sphingolipids and induce degeneration of sensory organs. The study is quite complete, but there are some serious weaknesses that preclude publication. If properly revised, the study can be published, as it will make important contribution to the field. The authors should consider the following points, when revising their manuscript:

We thank the reviewer for their recognition of the strengths of the manuscript, and for the care and constructive approach taken in their reviewing.

Title: The title is a bit lengthy, the authors should try to revise.
Revised, it is now 'A Saposin deficiency model in Drosophila: lysosomal storage, progressive neurodegeneration and sensory physiological decline' and we hope that this meets with approval.

- Pg. 6, para 2: The authors should clarify which type of images/staining was used to quantify vacuoles. *Done. Methods 'under light microscopy'*

- Pg. 11, para 2: The images showing dSap-r expression in organs other than the nervous system should be included in the main figures, because this information is an important element of the characterization.
We prefer to keep the expression data for other organs to the supplemental. The major issue with saposin-deficiency patients is neurodegeneration, and this is where we have focused our characterisation. Expression outside of the nervous system is important, but given the impermeability of the blood brain barrier, not critical to our analysis as presented.

- Pg. 13, para 2: The term "vacuolisation" appears is a bit ambiguous and misleading. Vacuoles are structures located within cells that are surrounded by a membrane. Is this what the authors observe? Or do they mean loss of groups of cells? The authors must clarify this important point using appropriate terms.
*In the Drosophila field this is a common term and characteristic of neurodegeneration in flies since it was identified as a phenotype by late Seymour Benzer. This phenotype is reflected in the names of some of the very informative neurodegeneration mutants such as 'spongecake', 'eggroll', 'vacuolar peduncle', 'bubblegum' and 'swiss cheese'. Indeed, in a paper from Mel Feany's lab, (Wittman et al., (2001) Science, 293, 711-714) the presence of vacuolisation in the absence of tauopathy in a fly tau expression model is taken as evidence for neurodegeneration, the key finding of the paper. There are many examples, we cite two in the text. We have however modified the text to clarify: '*In *Drosophila*, vacuolisation of the brain, the appearance of clearances within the neural tissue, is a hallmark of neurodegeneration (27, 20)'

- Pg. 14, para 2: The choice of the Arl-8 protein must be explained. Is this a standard marker for lysosomes that accumulates in lysosomal diseases?
We have limited markers for lysosomes in Drosophila, and we wanted an independent marker in addition to CathL. Arl8, as we have cited, is known to localise to the lysosome, it has not been used previously in the lysosomal storage disease context. We are of the opinion that, as a protein known to associate with lysosomes, it is indicative of lysosomal dysfunction and in this context is informative. The follow-up experiment with CathL supports our conclusion of lysosomal dysfunction.

- Pg. 14, para 2 and 3: The concluding statements are rather vague, they should be replaced. The authors' phenotypic description does not allow for solid conclusions of what is really going on in their mutants.
We have modified the paragraphs to use the formulations 'indicated' and 'suggests'.

- Pg. 15, para 2: The term "multivesicular bodies" is often used as a synonym for late endosomes having a more or less defined size range. A question is whether the MVBs observed by the authors represent late endosomes or some pathologic accumulation of vesicular material within or not membrane-delimited areas.
A key point made by the reviewer here is 'pathologic'. What we are saying, and I think we do so clearly, is that the material we see in the dSap-r mutants is similar to that seen in patient material. We are consistent with the lysosomal storage disease literature in referring to these structures by these terms, in that they resemble MVBs and this is the point we are trying to make. Nonetheless we have modified the text to now describe the MVBs as 'enlarged' in the pathologic state.

A more careful qualitative analysis of the ultrastructural changes is clearly required.

Respectfully, we are in disagreement. We have always felt that if this qualitative analysis were to give us any clear insight into the Sap-r mutants or the saposin deficiency condition, then we would agree with the reviewer and do this analysis, but at the level of TEM ultrastructure we do not think that this would be helpful or mechanistically insightful. To our knowledge such an analysis for other lysosomal storage diseases has not been informative.

Moreover, the meaning of the sentence "The ultrastructural nature..." is a bit unclear. What does accumulate in these these ultrastructurally defined structures? A recent study on NPC showed lipid accumulation in these multilamellar bodies (Demais et al., 2016 PMID: 27466344. Is this happening here as well?

Given the recent nature of this publication, July 2016, we have not had the opportunity to carry out such an analysis. Until the publication of this paper the nature of the multilamellar inclusions has been an assumed to be lipid, of late endosomal and phagosomal origin and we have worked with this common limited understanding of these structures that has been until the publication of this paper, a limitation in the field.

- Pg. 16, para 2 and elsewhere: This paragraph exemplifies a major weak point of the ms: the ultrastructural phenotype is described in several paragraphs and represented in distinct figures (Figs. 3-6). This is confusing and prevents a thorough appreciation of the changes. The authors should revise the presentation of the results and for example present ultrastructural observations in one paragraph with one or two figures. The same argument applies for physiologic/behavioral/life span changes.

We have brought the 'storage' data together in one figure, and the physiological data (climbing, electrophysiology) in another. We have kept the lifespan separate, as we feel this makes an early statement in the paper about premature death in the mutants, and the flow of the paper is then, early death to neurodegeneration to physiological deficits.

- Pg. 16, para 2: The authors must indicate where in the fly nervous system these changes occur. This is important for the future use of their model. *Done*

- Pg. 16, para 2: The images shown in supplementary fig 2 should be added to a main figure.
We respectfully disagree, we prefer to have this minor point in the supplemental figures

- Pg. 16, para 4, pg. 17, para 1: The general description of the ERG technique should be shortened or moved to the Material/Methods section. *Done.*

- Pg. 17, para 2: The statement "The ... potential deteriorated to 46% of..." is odd: why is the change compared to a different age rather than to the level in control mice of the same age?
In the previous sentence we state: 'ERG recordings in 5-day-old dSap-r^{C27}/Df mutants were not significantly different from controls in all components measured'.

- Pg. 17, para 3: The authors should revise the last sentence, because its meaning is not clear. *Done*

- Pg. 18, para 2: The impressive effects of CalX overexpression on ERGs raise the question, how CalX affects the life-span of dSap-r mutant mice. The authors should provide these data. *The CalX expression is only targeted to the fly eye via the NINAE promoter in this experiment, so we do not feel that this requested data would be informative.*

- Pg. 19, para 2: Given the expression of dSap-r in the reproductive system, the author should provide information on the fertility of the dSap-r mutant flies. Again, this is important for future use of this strain. *The dSap-r mutant stocks are kept as heterozygotes in trans to a balancer chromosome, and are generated for each experiment via a cross. Our characterisation has been focused on the nervous system, the key tissue affected by the disease; we feel that the addition of fertility information is not necessary or informative for our understanding of the disease, particularly as most patients with saposin deficiency don't normally reach reproductive age.*

- Pg. 20, para 3: Regarding their statement that "A similar degeneration in sensory function is observed...", the authors should cite previous studies showing retinal defects in NPC mice (Claudepierre et al., 2010 PMID: 19883762; Yan et al., 2014 PMID: 2547275; Palladino et al., 2015 PMID: 26458950). *Done.*

- Pg. 21, para 3, and elsewhere: The comparison with NPC should be limited to a few points. Although both diseases are classified as sphingolipidoses, it is not clear how much the mechanisms of neurodegeneration overlap. More important are probably the implications for saposin deficiency in humans.
We recognise this point, though we find it stands in contradiction to the

reviewer's previous point.

- Pg. 32: The lipid levels in the different fly mutants should be shown as column plots of normalized levels (see Fig. 4D, E) data rather than in the categorized table form which is not really very informative. Conditions, where no data are available (white cells in table), can be left out.
We agree with the reviewer and have added two new graphs for the lipid quantification section (now in Figure 5H and I). We have removed the table from the manuscript.

- Fig. 1: The micrographs should be enlarged, the labels are very hard to read. *Done*

- Fig. 2: The life-span plots are confusing. The different lines are hard to discriminate, and the difference between the three neuron Gal4 plots remains unclear. The authors should revise this presentation. *Done*

- Fig. 4: The results shown in A should be properly quantified using at least 3 preparations. *We have added this data. A statistical analysis shows great variability (error bars are large) for the three experiments and thus generates a non-significant effect. However in each experiment there is a clear increase in both Arl8 and CathL that is evident for all three biological repeats. We therefore feel that the increase is consistent and quantifiable.*

- Fig. 6: The micrographs in A should be enlarged. ERG data should be presented in a separate figure, possibly with other physiologic/behavioral data. The recording traces should be shown at a more compressed time scale to save some space. The plots shown in part B, left and D could be combined to save space and to avoid duplicate representation of results (e.g. C27/df).
We have combined the ERG data with the other physiological/behavioural data as suggested. Removal of the retinal degeneration micrographs provided extra space for the ERG data, therefore, we felt space-saving strategies were no longer required.

Minor points
- Pg. 1: The numbers representing author affiliations are ambiguous and must be corrected. *Done*
- Pg. 2: The phrase "hydrolases in the degradation" should be replaced by "hydrolases mediating the degradation" *Done*
- Pg. 2: The phrase "causing an absence" raises the question whether this is always true: is it the absence or impaired function. The authors should use a more precise statement. *Done*
- Pg. 3, para 1: The authors should provide OMIM codes to ease access to the relevant diseases. *Done*
- Pg. 3, para 3: Avoid double brackets "...NPC))". *Done*
- Pg. 6, para 1: The title of this paragraph ("head sectioning") should be replaced by a more appropriate term. *Done*
- Pg. 6, para 3: It should read "semi-thin". *Done*
- Pg. 9, para 1: "n=2" Numbers of observations (here and elsewhere) should be moved to the Results. *Done*

- Pg. 11, para 4: The sentence starting with "To assess the effect of each..." is a bit unclear and should be rewritten. *Done*
- Pg. 15, para 4. Change "We do not" to past tense. *Done*

***Highlights**

Highlights, Hindle et al.,

Drosophila model of PSD recapitulates neurodegenerative phenotype of human PSD

Preferential degeneration of sensory regions correlates with loss of sensory function

Sphingosine levels rise with age with an imbalance in sphingosine/ceramide ratios

Genetic interaction with the Na+/Ca+ exchanger points to a calcium regulation deficit

A Saposin deficiency model in *Drosophila*: lysosomal storage, progressive neurodegeneration and sensory physiological decline

Comment [SS1]: Deleted: and defective calcium homeostasis

Samantha J. Hindle[1,3], Sarita Hebbar[2,4], Dominik Schwudke[2,5], Christopher J. Elliott[1] and Sean T. Sweeney[1*]

[1]Department of Biology, University of York, York, YO10 5DD, U.K.

[2]National Centre for Biological Sciences, Tata Institute of Fundamental Research, Bangalore, Karnataka, 560065, India

[*]**Correspondence:** Sean T. Sweeney, Department of Biology, University of York, Wentworth Way, Heslington, York, YO10 5DD, U.K. email: sean.sweeney@york.ac.uk Tel: 01904 328537 Fax: 01904 328505

Present address:

[3]Department of Anesthesia and Perioperative Care, Genentech Hall, 600 16th Street, University of California San Francisco, San Francisco, CA.

[4]Max Planck Institute of Cell Biology and Genetics, Dresden, 01307, Germany

[5]Research Center Borstel, Leibniz-Center for Medicine and Biosciences, Borstel, 23845, Germany

Abstract

Saposin deficiency is a childhood neurodegenerative lysosomal storage disorder (LSD) that can cause premature death within three months of life. Saposins are activator proteins that promote the function of lysosomal hydrolases that mediate ~~in~~ the degradation of sphingolipids. There are four saposin proteins in humans, which are encoded by the *prosaposin* gene. Mutations causing an absence or impaired function of individual saposins or the whole prosaposin gene lead to distinct LSDs due to the storage of different classes of sphingolipids. The pathological events leading to neuronal dysfunction induced by lysosomal storage of sphingolipids are as yet poorly defined. We have generated and characterised a *Drosophila* model of saposin deficiency that shows striking similarities to the human diseases. *Drosophila saposin-related* (*dSap-r*) mutants show a reduced longevity, progressive neurodegeneration, lysosomal storage, dramatic swelling of neuronal soma, perturbations in sphingolipid catabolism, and sensory physiological deterioration. Our data suggests a genetic interaction with a calcium exchanger (Calx) pointing to a possible calcium homeostasis deficit in *dSap-r* mutants. ~~We have also revealed a genetic interaction with a calcium exchanger (CalX), suggesting that calcium homeostasis may be altered in saposin deficiency.~~ Together these findings support the use of *dSap-r* mutants in advancing our understanding of the cellular pathology implicated in saposin deficiency and related LSDs.

Keywords: prosaposin deficiency; sapsosin; lysosomal storage disease; Drosophila; neurodegeneration; sphingolipids

Abbreviations:

PSAP	Prosaposin
ERG	electroretinograms
LSD	lysosomal storage disease
NPC	Niemann Pick type C
GFP	green fluorescent protein
RT-PCR	reverse transcription PCR
TEM	transmission electron microscopy
MVB	multivesicular body

MLB	multilamellar body
HSAN1	Hereditary sensory and autonomic neuropathy type 1

Introduction

Saposin deficiency is an autosomal recessive lysosomal storage disorder (LSD) that is typically associated with severe, age-dependent neurodegeneration and premature death during early childhood. In humans there are four saposins (saposins A – D), which are encoded by the *prosaposin* gene ~~1~~(Furst et al., 1988; Nakano et al., 1989; O'Brien et al., 1988). The mature, active saposins are produced by cleavage of the prosaposin precursor during passage through the endosomes to the lysosomes; this function is primarily performed by Cathepsin D (Hiraiwa et al., 1997). Once in the acidic lysosome environment, saposins act as activator proteins and promote the function of hydrolases involved in sphingolipid degradation (Azuma et al., 1994; Berent and Radin, 1981; Morimoto et al., 1989; Vogel et al., 1987; Yamada et al., 2004). Mutations in *prosaposin* therefore cause a primary accumulation of sphingolipid species in the lysosomes. The location and severity of the *prosaposin* mutation dictates the number of saposins that are affected and hence the degree of sphingolipid accumulation and age of lethality. Mutations abolishing the *prosaposin* start codon result in an absence of prosaposin and therefore all 4 saposins (OMIM #611721); this causes the most severe pathology and individuals present with severe neurodegeneration at birth and die within 4 months (Elleder et al., 1984; Harzer et al., 1989; Hulkova et al., 2001). Of the single saposin disorders, saposin A deficiency is the most severe and results in death at 8 months old ((Spiegel et al., 2005); OMIM #611722), whereas the mildest of the saposin C mutations cause non-neuronopathic disorders with relatively mild symptoms until the fourth decade of life ((Tylki-Szymanska et al., 2007); OMIM #610539). No single saposin D deficiencies have been reported in humans.

Because each saposin generally promotes the function of a specific sphingolipid hydrolase, the single saposin deficiencies resemble the pathology caused by mutations in their cognate hydrolase (e.g.

(Christomanou et al., 1986); reviewed in (O'Brien and Kishimoto, 1991)); total prosaposin deficiency encapsulates many aspects of the single saposin deficiencies but to a more severe degree (Elleder et al., 1984; Harzer et al., 1989; Hulkova et al., 2001).

The sphingolipdoses form the largest group of LSDs, yet to date only one sphingolipidosis, (Niemann-Pick Type C (NPC),) has been modelled in *Drosophila* (Fluegel et al., 2006; Huang et al., 2005; Huang et al., 2007; Phillips et al., 2008). To broaden our understanding of the sphingolipidoses, and to help identify pathological events subsequent to sphingolipid storage, we generated a *Drosophila* model of saposin deficiency. The *Drosophila Saposin-related* (*dSap-r*) locus encodes a protein predicted to contain eight saposin-like domains, each containing the classic six-cysteine arrangement found in all mammalian saposins. Characterisation of *dSap-r* mutants revealed pathology similar to that of the human disorders, including reduced longevity, progressive neurodegeneration, aberrant sphingolipid levels, and physiological deterioration; all hallmark signs of lysosomal storage. Our analysis reveals a genetic interaction with the Na+/Ca+ exchanger, CalX, and suggests a deficit in calcium regulation in the *Drosophila* model of saposin deficiency.

Materials and Methods

Identification of *Drosophila Sap-r*

A blastp search (NCBI; www.ncbi.nlm.nih.gov) was performed to identify the *Drosophila melanogaster* prosaposin (PSAP) homologue. The entire *Homo sapiens* PSAP protein sequence (CAG33027) was used to search the *D. melanogaster* protein database. Standard blastp assumptions were applied. A reciprocal search was performed, using the *D. melanogaster* d-Sap-rPA sequence to blast the *H. sapiens* protein database, to ensure the correct homologue was identified.

Identification of *Drosophila Sap-r* monosaposins

To identify the putative monosaposins encoded by the *dSap-r* gene, each human monosaposin sequence (RCSB Protein Data Bank entries 2DOB, 1N69, 2GTG, 2RB3) was aligned against the full-length dSap-rPA sequence using the bl2seq tool at NCBI. The *H. sapiens* and *D. melanogaster* monosaposins were aligned using default settings in ClustalX.

***Drosophila* stocks.** All experimental crosses were grown on maize-meal fly food at 25°C. Newly eclosed flies were transferred to standard yeast-sucrose-agar fly food. The wild type (+/+) control for all experiments was w^{1118} crossed to Canton-S. The *dSap-r*^{PBac} and Df(3R)*tll-e* (subsequently referred to as a 'deficiency' or Df, a large deletion of the genomic region encompassing the *dSap-r* locus~~Df~~) stocks were from the Bloomington stock centre and the *dSap-r*^{NP7456} stock was from the Kyoto stock centre. The *dSap-r*^{C27} deletion was generated for this study by mobilising the *P*-element from the *dSap-r*^{NP7456} parent line. The *UAS-dSap-r* transgenic stock was generated for this study as follows.~~-~~ Briefly, pUAST-*dSap-r* was generated by excision of *dSap-r* cDNA from the pOT2 vector (clone GH08312, BDGP Gold collection), using XhoI and EcoRI followed by ligation into the pUAST vector. pUAST-*dSap-r* was microinjected into w^{1118} embryos with helper plasmid Δ*2-3*. *UAS-mCD8GFP* and 1407-GAL4 stocks were kindly provided by Andreas Prokop (University of Manchester, UK).

Longevity. Newly eclosed flies were collected in separate-sex vials of approximately 10 flies/vial and aged at 29°C ~~(n>100 flies, unless otherwise stated)~~. Flies were transferred to fresh food every 2-3 days and the number of surviving flies recorded. Longevity was plotted as the percentage of Day 0 flies alive each subsequent day.

Immunohistochemistry. For the *dSap-r* expression pattern, third instar larvae ~~(n>5)~~ were dissected and fixed in 3.7% formaldehyde/PBS for 10 min, followed by 3 x 5 min washes in 0.1% PBST (PBS with 0.1% Triton X-100). Larvae were labelled overnight at 4°C with mouse anti-repo-8D12 or mouse anti-elav-9F8A9 diluted in PBST (1:50; Developmental Studies Hybridoma Bank, University of Iowa). Washes were performed as above, followed by

incubation for 2 h at RT in Cy3-conjugated goat anti-mouse IgG (1:200; Jackson ImmunoResearch). Larvae were washed (as above) and left in 70% glycerol/PBS for 1 – 2 h before mounting in Vectashield (Vector Laboratories). To label lysosomes, aged adult brains were dissected in 4% paraformaldehyde/PBS and transferred to fresh fixative for 20 min ~~(n>8)~~. Brains were washed 3 x 15 - 20 min in 0.3% PBST followed by incubation overnight at RT with rabbit anti-Arl-8 (1:500; kindly provided by Debbie Smith, University of York, U.K) and mouse anti-elav (1:50). Brains were washed as above, followed by incubation for 3 h at RT in FITC-conjugated goat anti-rabbit IgG and Cy3-conjugated goat anti-mouse IgG (1:200; Jackson ImmunoResearch). Brains were washed and mounted in Vectashield. All images were acquired using a Zeiss LSM 510 meta Axiovert 200M laser scanning confocal microscope.

~~Head sectioning.~~Fly head processing for light microscopy. Aged flies were briefly dipped in 30% ethanol before being submerged in fixative (4% paraformaldehyde, 1% glutaraldehyde in 0.1M sodium phosphate buffer, pH 7.4) and pinned through the abdomen. The proboscis and accessible air sacs were rapidly removed from the heads. Heads were transferred to glass vials containing fresh fixative and were vacuum treated to remove trapped/adherent air. Vacuum-treated heads were incubated in fresh fixative overnight at 4°C. All incubations were performed on a rotating wheel, unless otherwise stated. Heads were washed 3 x 10 min in 0.1M sodium phosphate buffer and post-fixed in 1% OsO_4 for 1 h. Following washes in 0.1M sodium phosphate buffer (3 x 10 min) and dH_2O (3 x 10 min), heads were dehydrated in an acetone series (30%, 50%, 70%, 90%, 3x 100%; 20 min each). Heads were incubated in increasing concentrations of Spurr's resin:acetone (25%, 50%, 75%, 95%, 2x 100% [at 37°C]; 45 min each) followed by incubation in 100% resin overnight at 4°C without rotation. Heads were embedded in Spurr's resin (Spurr, 1969) for 24h at 70°C. Three semi-thi~~ck~~ serial sections (1.0 µm; Leica Ultracut UCT) were taken every 10 – 20 µm until the desired depth was reached. Sections were dried onto glass slides, stained with 0.6% toluidine blue in 0.3% sodium carbonate on a hot plate (80°C) and rinsed with

dH_2O. Sections were imaged using a Zeiss Axiovert 200 microscope equipped with a Zeiss AxioCam HRm camera.

Quantification of vacuole number. Vacuoles, transparent clearings in the neuronal tissue, were quantified manually under light microscopy for the antennal lobes and the visual system (eye, lamina, medulla, lobula and lobula plate) from 3 serial sections per fly head ~~(n≥3)~~. The sections were matched for depth through the head. Vacuoles were counted from both sides of the head. ANOVA statistical tests were performed using SPSS software (IBM Corp., USA).

Transmission electron microscopy. After reaching the desired depth by semi-thin~~ck~~ sectioning, the same embedded heads used for light microscopy were sectioned for transmission electron microscopy ~~(n=3)~~. Ultrathin sections (60 – 70 nm) were collected on 200 and 400 mesh coated grids, treated with uranyl acetate in 50% ethanol for 10 min and submerged in dH_2O to wash. Sections were stained with lead citrate for 10 min in the presence of sodium hydroxide pellets, followed by washing in dH_2O. Images were captured using analysis software on a TECNAI G^2 (Version 2.18) transmission electron microscope (120 kV).

Neuronal soma area quantification. All TEM micrographs were imaged from the cortex surrounding the antennal lobes (see lower panel in Fig. 3A). Neuronal soma area was quantified using ImageJ software. The soma and nuclear boundary of each neuron were demarcated and the area calculated by first inputting the number of pixels per micron then using the ImageJ area measurement tool. Neuronal soma area were normalised to nuclear area ~~(n=3 flies)~~. Pseudocolour images were produced using Adobe Illustrator CS4. Student's t-tests were performed in Microsoft Excel to determine statistical significance.

Lipid extraction and lipidomics analyses. Female adults of the required genotypes were collected on emergence and aged for 5 days. Three brains/biological replicate were dissected in PBS, flash-frozen in 20%

methanol using liquid nitrogen, and stored at -80°C until lipid extraction was performed. Brain samples were homogenized and extracted according to the methyl-tert-butyl ether extraction method (Matyash et al., 2008). All lipid standards were added to the homogenates prior to extraction (Supplemental Table 2). After phase separation, the organic phase was used for lipidomics and the aqueous phase was processed for determining total protein content using the bicinchoninic acid (BCA) assay (BCA1 kit, Sigma).

For Mass Spectrometry measurements, the samples were dissolved in 100 µl methanol containing 0.1% ammonium acetate and subsequently analyzed using a flow-injection system at a flowrate of 1 µl/min and 5 µl sample injection. Negative and positive ion mode spectra were acquired with a LTQ-Orbitrap XL (Thermo Fisher Scientific, Germany) equipped with an Agilent 1200 micro-LC system (Agilent Technologies, USA) and a Nanomate Triversa utilizing 5 µm ID ESI-chips (Advion, Biosciences, USA).

In the negative mode Phosphatidylinositol (PI), Phosphatidylethanolamine (PE), Polyethylene oxide (PE-O), Lysophosphatidylethanolamine (LPE), Phosphatidylcholine (PC), Ceramide phosphorylethanolamine (CerPE), Phosphatidylserine (PS), Phosphatidylglycerol (PG) could be identified according to their accurate mass (Schwudke et al., 2011). For PS, the specific neutral loss of 87Da was monitored in the linear ion trap and used for quantification. In the positive mode Sph 14:1, Ceramides and HexCeramides were monitored with MS^3 in the linear ion trap using the long chain base related fragment ions. All MS^3 for quantifying sphingolipids were analyzed using Xcalibur software 2.07 (Thermo Fisher Scientific, Germany) while all other analyses were performed using LipidXplorer 1.2.4 (Herzog et al., 2011). Absolute levels of individual lipid species (picomol/ug protein) were summed to arrive at lipid class abundances. A minimum of 4 replicates were used for the analyses. Prism 6 software (Prism Software Corp., USA) was used for graph representation and for determining significant differences applying ANOVA coupled with post-hoc Bonferroni tests.

RT-PCR. RNA was extracted from third instar larvae using a QIAGEN RNeasy kit, according to manufacturer's instructions. RNA was treated with

DNase prior to cDNA generation. The following primers were used for RT-PCR:
5'TCCTACCAGCTTCAAGATGAC3' (rp49 Forward),
5'GTGTATTCCGACCACGTTACA3' (rp49 Reverse),
5'GCAACTGCAACCTGCTTTCC3' (dSap-r Forward) and
5'GCATCGTTTCCACCATGTCA3' (dSap-r Reverse).
All PCR reactions using *rp49* and *dSap-r* primers were performed with an elongation time of 1 min, an annealing temperature of 50°C and 55°C, and a cycle number of 25 and 35, respectively. *dSap-r* primers anneal downstream of the $dSap\text{-}r^{C27}$ deletion, but upstream of the $dSap\text{-}r^{PBac}$ insertion.

Western blotting. Soluble protein was extracted from aged flies using 10 µl lysis buffer per fly (150 mM NaCl, 20 mM Tris-HCl, pH 8.0, 2 mM EDTA, 0.5% (v/v) NP-40, 1 complete mini protease inhibitor cocktail (Roche)). A standard western blotting procedure was followed including blocking in 5% milk/TBST (Tris buffered saline supplemented with 0.1% (v/v) Tween-20) followed by incubation in primary then secondary antibody diluted in 5% milk/TBST. Washes were performed using TBST. The following antibodies were used: rabbit anti-Arl-8 (1:2000; kindly provided by Debbie Smith, University of York, UK), mouse anti-β-tubulin E7 (1:100; Developmental Studies Hybdridoma Bank, University of Iowa, USA), mouse anti-cathepsin-L (1:250; R&D Systems), hoseradish peroxidase (HRP)-conjugated goat anti-rabbit (1:6000; Sigma) and HRP-conjugated goat anti-mouse (1:10000; Sigma). Bands were visualised using ECL reagent (GE Healthcare, UK) and developed using a Xograph machine. Densitometry was performed using ImageJ. Band intensities were first normalized to the tubulin control and then to the 5d old wild type control. ~~n=2~~

Behavioural analyses. The climbing ability of female flies was assessed by tapping cohorts of 5 flies to the bottom of a 100 ml glass measuring cylinder and video recording the climbing response over 45 s. The data were analysed by quantifying the climbing speed of each fly over 10% intervals of the measuring cylinder. The maximum speed for each fly was used to calculate the average speed per genotype. The same flies tested at 5-days old were re-

tested at 22-days old, when possible ~~(n>20 flies)~~. ANOVA statistical tests were performed using SPSS software (IBM Corp., USA).

Electroretinograms. ERGs were performed as described in (Hindle et al., 2013). Briefly, aged female flies were left to climb a trimmed 200 µl pipette tip and were blown to the end leaving the fly head protruding. The fly was fixed into position with nail varnish. Glass electrodes were pulled and filled with *Drosophila* Ringer solution (0.13 M NaCl, 4.7 mM KCl, 1.9 mM $CaCl_2$) (34). A recording electrode was placed against one eye and a reference (earth) electrode placed against the proboscis using micromanipulators. The flies were dark-adapted for 5 min (Fig. 6B - C) or 2 min (Fig. 6D - E). ERGs were recorded in response to 5 x 750 ms blue light pulses with 10 s intervals. Light pulses were provided by a blue LED lamp (Kingbright, Taiwan) controlled by DASY*Lab* software (Measurement Computing Corp., USA). ERGs were analysed using DASY*View* software (customised software, C. Elliott) ~~n≥10 flies, unless otherwise stated.~~

Supplemental Methods

Formatted: Keep with next

Epifluorescence. Organs were dissected from adult flies in PBS and, in some cases, stained with DAPI. Organs were imaged using a Zeiss stereomicroscope equipped with an Axiocam MRc5 camera, a Neolumar S 1.5x FWD 30 mm lens and a HBO 100 mercury lamp.

Results

dSap-r has homologous sequence structure and similar expression pattern to mammalian prosaposin.

The *Drosophila* prosaposin (PSAP) homologue (Saposin-related; dSap-r) was identified by a BLAST screen using the complete human PSAP protein sequence (blast E value 4e-36). The *dSap-r* locus is located at band 100A7 of the right arm of the third chromosome. There are two predicted transcripts for *dSap-r* (*dSap-r RA* and *dSap-r RB*); *dSap-r RB* appears to be an in-frame truncation of *dSap-r RA* (Fig. 1A).

A bl2seq alignment of each human monosaposin (Sap A-D) with the dSap-r protein revealed eight homologous *Drosophila* saposins (dSaps 1-8). Each dSap contained the six conserved cysteine residues critical for saposin function (Fig. 1B). Five of the dSaps also contained a potential glycosylation signal between the second and third cysteines, previously shown in mammals to be necessary for correct saposin folding and function (Hiraiwa et al., 1993b).

Saposin proteins are expressed in the mammalian nervous system and their loss usually causes severe neurodegeneration (Sun et al., 1994; Van Den Berghe et al., 2004; Yoneshige et al., 2009). We therefore investigated the expression pattern of dSap-r in the nervous system. The *dSap-r*^{NP7456} GAL4 enhancer-trap insertion was used to drive a membrane localised GFP reporter (mCD8GFP) in a dSap-r-specific expression pattern. Third instar larvae were dissected and stained with either a glial or neuronal antibody (α-repo or α-elav, respectively). The membrane GFP reporter localised around repo-positive nuclei, suggesting that *dSap-r* is expressed in glial cells (Fig. 1C). The GFP reporter was also shown to faintly surround elav-positive neuronal nuclei, however this is likely to represent expression in glial cells that surround the neuronal cell bodies. To confirm whether *dSap-r* is expressed in neurons, a nuclear GFP reporter (eIF4AIII:GFP) was driven by the *dSap-r*^{NP7456} element. No colocalisation was found between the nuclear GFP reporter and neuronal nuclei, suggesting that neurons have no or very little *dSap-r* expression (Fig 1C). The nuclear GFP colocalised with the glial nuclear marker, further confirming *dSap-r* expression in glia.

In mammalian visceral organs, *prosaposin* is expressed ubiquitously at low levels; however moderate to high expression levels are found in the jejunum and tubular epithelial cells in the kidney cortex, epithelial cells of the oesophagus, pancreatic duct and bile duct, and the hepatocytes of the liver (Sun et al., 1994). PSAP has also been shown to promote spermiogenesis and fertility (Amann et al., 1999; Hammerstedt, 1997). Using the mCD8GFP reporter in conjunction with the *dSap-r*^{NP7456} enhancer-trap element, *dSap-r*

was shown to be highly expressed in the reproductive system, the digestive system, Malpighian tubules (*Drosophila* kidney), and the fat bodies (*Drosophila* liver and adipose tissue) of the adult fly (Fig. S1).

The similar expression pattern of dSap-r and mammalian saposins in cells of the nervous, reproductive, digestive, and renal systems, and the liver is suggestive of conserved functions, and therefore supports the use of *Drosophila* to model these disorders.

***dSap-r* mutation causes a reduced longevity ~~and age-dependent deterioration of locomotion~~.**

Patients with saposin deficiency die prematurely, usually within the first decade of life. To test whether *dSap-r* mutants also die prematurely, we first generated deletions of the dSap-r locus via an imprecise P-element mobilisation strategy. The *dSap-r*^{C27} allele is a deletion of the first two exons of the *dSap-r* locus (Figure 1A). We also identified a PiggBac transposon insertion, *dSap-r*^{PBac}, in the 4th exon of the dSap-r locus (Figure 1A). To assess the ~~*effect of* dSap-r~~ transcript levels in ~~each~~ the *dSap-r* ~~mutation~~ mutants~~on *dSap-r* transcript levels~~, RT-PCR was performed ~~on transheterozygous combinations of these two alleles, and combinations of these alleles in trans to a deficiency chromosome uncovering the *dSap-r* locus~~ (Fig. 1A and 2C). The *dSap-r* transcript was almost undetectable in *dSap-r*^{C27}/Df mutants and is likely to reflect *dSap-rRB* levels, as the *dSap-rRA* start site is deleted in this mutant. In contrast, *dSap-r* transcript levels in the *dSap-r*^{PBac} mutant were indistinguishable from wild type; however, the *dSap-r* primers were designed to anneal upstream of the *dSap-r*^{PBac} insertion. Production of saposins from the dSap-r locus prior to the PBac transposon insertion is therefore possible.

Next we tested the effect of these mutant *dSap-r* alleles using~~Using our *dSap-r* mutants, a~~ longevity assay~~s was performed~~. Each of the three *dSap-r* mutant allelic combinations caused a reduction in longevity compared to wild type flies (Fig. 2A). Median survival for wild type flies was approximately 35 days, whereas 50% of *dSap-r* mutants survived only 6 days (*dSap-r*^{C27}/Df), 15

days (*dSap-r*$^{C27/PBac}$) or 18 days (*dSap-r*^{PBac}/Df). This suggests that the *dSap-r*^{C27} mutant allele is more severe than the *dSap-r*^{PBac} mutant allele. Taken together with the RT-PCR results, this suggests that the *dSap-r*^{C27} mutant allele is likely a strong loss-of-function mutation, whereas the *dSap-r*^{PBac} mutant allele may produce dSap-r protein with reduced or aberrant function.

To confirm that the *dSap-r* mutations were responsible for the reduced longevity, flies carrying a UAS-*dSap-r* transgene were generated to allow GAL4-driven rescue of *dSap-r* mutant longevity. Ubiquitous expression of *dSap-r* using either Act5c-GAL4 or tubulin-GAL4 resulted in lethality prior to third instar; we therefore used *dSap-r* expression driven by the neuronal 1407-GAL4 (Fig. 2A) or the glial repo-GAL4 (Fig. 2B)~~, either of which did not induce lethality,~~ for rescue experiments. Expression of *dSap-r* in neurons of all *dSap-r* mutant combinations resulted in a substantial rescue of longevity and in most cases longevity was equivalent to the transgene control. Glial *dSap-r* expression was only driven in the *dSap-r*$^{C27/PBac}$ mutants ~~only~~, due to greater genetic ease of repo-GAL4 recombination using the *dSap-r*^{PBac} mutant allele. Glial *dSap-r* expression ~~also~~ provided a substantial rescue of *dSap-r*$^{C27/PBac}$ mutant longevity, however, not to the same degree as the neuronal 1407-GAL4 expression. These results confirm that the reduced longevity in *dSap-r* mutants was due to *dSap-r* mutations.

~~During the longevity analysis it was observed that the *dSap-r* flies showed an age-dependent decline in locomotion; the 20+ day-old *dSap-r* mutants rarely climbed the vial during spontaneous activity. To quantify this loss of climbing behaviour, 5-day and 22-day-old female flies were tapped to the bottom of a measuring cylinder and their climbing response was captured by video for 45 seconds. Calculation of climbing speed revealed that the 22-day-old *dSap-r*^{C27}/Df mutants were only able to climb at 5% of their 5-day-old speed compared to maintenance of 36% of 5-day climbing speed for the *dSap-r*^{C27}/+ controls. The *dSap-r*$^{C27/PBac}$ mutants showed an intermediate phenotype maintaining 16% of their 5-day climbing ability at 22-days old. These data confirm an age-dependent deterioration of climbing behaviour in the *dSap-r* mutants (Fig. 2D).~~

Age-dependent neurodegeneration in *dSap-r* mutants.

~~The reduced longevity and age-dependent deterioration of locomotion in *dSap-r* mutants is suggestive of~~The Saposin-deficiencies are primarily classed as progressive neurodegenerative disorders~~on~~. Therefore, we next assessed whether our *dSap-r* model showed age-dependent neurodegeneration. In *Drosophila*, vacuolisation of the brain, the appearance of clearances within the neural tissue is a hallmark of neurodegeneration (Dermaut et al., 2005; Phillips et al., 2008), which can be quantified from 1 μm tissue sections at the light microscopy level. Horizontal sections were taken from 5-day and 22-day-old fly heads and stained with toluidine blue. Vacuolisation was specifically observed in regions of sensory function, mainly the antennal lobes, the eye, and optic lobes (Fig. 3A). Vacuole number was quantified for these sensory regions (Fig. 3B & C) where we observed that vacuole number in most 5-day-old *dSap-r* mutants was not significantly different from controls, with the exception of limited vacuolisation observed in the antennal lobes of the *dSap-r*^{C27}/Df mutants. As the flies aged, the number of vacuoles increased in all *dSap-r* mutants, indicative of progressive neurodegeneration. In the visual system, vacuole number increased by 4 – 18 fold in the *dSap-r* mutants compared to less than a 1.5 fold increase in the controls. In the olfactory system (antennal lobes), the controls showed a modest 1.5 – 3-fold increase in vacuole number. In contrast, the *dSap-r*^{PBac}/Df and *dSap-r*$^{C27/PBac}$ mutants showed a massive 6-fold and 16-fold increase in vacuole number, respectively. Although the *dSap-r*^{C27}/Df mutants showed the greatest number of vacuoles at 22-days old, the increase was only 3-fold due to the increased severity of vacuolisation at 5-days old.

***dSap-r* mutants have age-dependent lysosomal storage defects**

LSDs are characterised by lysosomal dysfunction leading to the storage of undegraded material in the lysosomes (Jardim et al., 2010). Therefore, to assess the degree of lysosomal dysfunction and storage in *dSap-r* mutants, western blotting was performed using antibodies for two lysosomal ~~antibodies~~proteins: ~~anti-~~Arl-8 and ~~anti-~~Cathepsin-L.

Formatted: Keep with next

Arl-8 is an Arf-like GTPase that localises to the lysosomes (Hofmann and Munro, 2006). Cathepsin-L is a lysosomal enzyme that is synthesised as an inactive precursor andthat is cleaved in the lysosome to form its mature, active form (Erickson, 1989). The Arl-8 antibody was used to probe a western blot containing soluble protein from 5-day and 22-day-old flies to investigate the degree of lysosomal storage in *dSap-r* mutants (Fig. 4A). In 5-day-old flies, Arl-8 levels were similar between wild type and *dSap-r* mutants. However, in 22-day-old *dSap-r* mutant flies, Arl-8 levels were increased compared to wild type and the 5-day-old samples (Fig. 4A). Similarly, an increase in the mature form of Cathepsin-L was found in all 22d old *dSap-r* mutants. This age-dependent increase in Arl-8 and mature Cathepsin-L storage is show by densitometry quantification, however these data did not reach significance due to a variability in the degree of storage in the *dSap-r* mutants. These datais suggests a trend ofn age-dependent dysfunction and accumulation of lysosomal material in *dSap-r* mutants and implies that lysosomes are more abundant and/or lysosomal enlargement/sweellingen in *dSap-r* mutants, which is consistent with the human disease.

To determine whether this increased abundance of Arl-8 is suggestive of general lysosomal dysfunction, western blot analysis was repeated using an antibody against a lysosomal enzyme (Cathepsin-L). Like all Cathepsins, Cathepsin-L is synthesised as an inactive precursor that is cleaved in the lysosome to form its mature, active form (30). Therefore, if lysosomal function is disturbed in *dSap-r* mutants, Cathepsin-L processing should be less efficient leading to an accumulation of the unprocessed, larger form. Western blot analysis of 5-day and 22-day-old lysates revealed an increase in both the unprocessed and processed forms of Cathepsin-L in all *dSap-r* mutants compared to age-matched controls, but no change in the ratio of unprocessed:processed Cathepsin-L (Fig. 4A). This supports the lysosomal storage phenotype indicatedshown by Arl-8 western analysis, but suggests that lysosomal function has not been completely perturbed.

In addition to western blotting, the Arl-8 antibody was used for immunohistochemistry on wild type and *dSap-r*^{C27}/Df mutant adult brains. An overall increase in fluorescence was observed in the aged *dSap-r* mutant brains, particularly in central brain regions and the antennal lobes (Fig. 4B). Together with our light microscopyical analysis of brain sections, this reveals that regions of severe neurodegeneration coincide with the regions of the CNS showing the most lysosomal storage.

***dSap-r*^{C27}/Df mutant CNS soma are enlarged with storage.**

To investigate this lysosomal storage defect further, we performed transmission electron microscopy on 22-day old *dSap-r*^{C27}/Df mutant antennal lobes, the same region where we saw the increased severity of neurodegeneration. We observed that *dSap-r*^{C27}/Df mutant neuronal soma were consistently and grossly enlarged with electron-dense storage material. To quantify this difference in soma size, the boundaries of each neuron were marked using ImageJ and the soma area measured (Fig. 5A). Measuring the average soma area revealed an almost 2.5-fold increase in *dSap-r*^{C27}/Df mutants compared to wild type (Fig. 5B). When normalised to nucleus area, the *dSap-r*^{C27}/Df mutant soma were almost 2-fold larger, suggesting that nuclear area is also increased in *dSap-r*^{C27}/Df mutant neurons (Fig. 5C). We also observed cell enlargement and increased storage in glial cells of the *dSap-r*^{C27}/Df mutant adult CNS (Supplemental Fig. 2).

As a common characteristic of LSDs is the accumulation of membranous storage material known as multilamellar bodies (MLBs) and enlarged multivesicular bodies (MVBs), w. We investigated whether the 22-day old *dSap-r*^{C27}/Df mutants carried showed these hallmark signs in the cortex surrounding the antennal lobes. Due to the severe degeneration occurring around the antennal lobes (Fig. 3A), this region of the brain was the main focus for ultrastructural analyses. Electron micrographs of 22-day-old *dSap-r*^{C27}/Df neurons revealed neurons with an abundance of electron dense storage material that hads a complex morphology; some regions were populated by electron-lucent droplets, some contained variable numbers of

MLBs, and others were densely packed with MVBs (Fig. 5D4C**)**. Electron micrographs also revealed an abundance of stored material in photoreceptor neurons of the fly retina (Fig. 5E), another sensory region of the nervous system that showed severe degeneration (Fig. 3A). This stored material had a similar morphology to that found in the antennal lobe neurons (Fig. 5D). High magnification images showed a variable phenotype in the rhabdomeres, the light responsive component of the eye. Most rhabdomeres showed massive accumulation of electron-dense material yet some were found to be structurally intact (Fig. 5E).

The ultrastructural nature of storage material in saposin deficiency patients and mammalian models has been shown to be highly variable, with the presence of MLBs, MVBs and electron-lucent droplets (Fujita et al., 1996; Harzer et al., 1989; Hulkova et al., 2001; Oya et al., 1998). The ultrastructural pathology observed in the *dSap-r* mutants is therefore consistent with the reported disease phenotype, which further supports the use of this model for investigating saposin deficiency.

~~Electron micrographs revealed an abundance of stored material in photoreceptor neurons of the fly retina (Fig. 6A), similar in morphology to that found in the antennal lobe neurons (Fig. 4C). High magnification images showed a variable phenotype in the rhabdomeres, the light responsive component of the eye. Most rhabdomeres showed massive accumulation of electron-dense material yet some were found to be structurally intact (Fig. 6A).~~

Sphingolipids accumulate in *dSap-r* mutant brains

To gain a greater insight into the nature of the stored material in *dSap-r* mutants, we performed mass spectrometry. As s~~S~~aposin deficiency leads to the accumulation of a complex array of sphingolipids and sphingolipid intermediates,~~.~~ ~~To~~ we determined the nature of sphingolipid perturbation in *dSap-r* mutants~~,~~ by~~we~~ monitoringed Hexosyl-Ceramides (HexCer), Ceramide phosphorylethanolamine (CerPE), Ceramide (Cer) and Sphingosine (the breakdown product of Ceramide;(Yuan et al., 2011)) in conjunction with a

lipidomic analysis of all major membrane phospholipids in the brain ~~(Supplemental Table 1)~~.

Brains from 5-day old flies revealed a consistent increase in sphingolipids ~~,(Supplemental Table 1)~~, particularly sphingosine, in all *dSap-r* mutants examined (Fig. 5F~~4D~~). Notably, comparison of the sphingosine:ceramide ratios in controls and mutants revealed a striking imbalance between these sphingolipid intermediates in the *dSap-r*$^{C27/Df}$ mutants (Fig. 5G~~4E~~). We d~~o~~ not observe a significant change in HexCer across the mutant combinations ~~(Supplemental Table 1)~~.

Changes in particular phospholipid classes were observed. However, unlike the sphingolipids, there is no specific and consistent trend for changes in phospholipid classes across the different *dSap-r* mutant combinations tested (Fig. 5H&I) ~~(Supplemental Table 1)~~.

Formatted: Comment Text

Formatted: Font color: Text 1

Formatted: Font color: Text 1

Formatted: Comment Text

~~***dSap-r*^{C27}/Df CNS soma are enlarged with storage.***~~

~~During ultrastructural analyses of the CNS we observed that *dSap-r*^{C27}/Df neuronal soma were consistently and grossly enlarged compared to wild type. To quantify this difference, the soma boundaries of each cell were marked using ImageJ and the soma area measured (Fig. 5A). Measuring the average soma area revealed an almost 2.5-fold increase in *dSap-r*^{C27}/Df mutants compared to wild type (Fig. 5B). When normalised to nucleus area, the *dSap-r*^{C27}/Df soma were almost 2-fold larger suggesting that nuclear area is also increased in *dSap-r*^{C27}/Df neurons (Fig. 5C). We also observed cell enlargement and increased storage in glial cells of the *dSap-r*^{C27}/Df adult CNS (Supplemental Fig. 2).~~

***dSap-r* mutants show progressive physiological decline**

After establishing that *dSap-r* mutants showed age-dependent neurodegeneration, we investigated the effect of *dSap-r* mutation on the physiological of the whole fly. We observed that the *dSap-r* mutant flies showed an age-dependent decline in locomotion; the 20+ day-old *dSap-r* mutants rarely climbed the vial during spontaneous activity. To quantify this loss of climbing behaviour, 5-day and 22-day-old female flies were tapped to the bottom of a measuring cylinder and their climbing response was captured

by video for 45 seconds. Calculation of climbing speed revealed that the 22-day-old *dSap-r*^{C27}/Df mutants were only able to climb at 5% of their 5-day-old speed compared to maintenance of 36% of 5-day climbing speed for the *dSap-* *r*^{C27}/+ controls. The *dSap-r*$^{C27/PBac}$ mutants showed an intermediate phenotype maintaining 16% of their 5-day climbing ability at 22-days old. These data confirm an age-dependent deterioration of climbing behaviour in the *dSap-r* mutants (Fig. 6A).

Loss of *dSap-r* function causes a deterioration of visual function

The decline of locomotor ability in *dSap-r* mutants could be due to a deterioration of motor neuron or sensory neuron function; however, wWe have shown that sensory regions of the brain, including the visual system, are particularly vulnerable to *dSap-r* mutation. To assess the effect of *dSap-r* mutation on the function of sensory neurons, we investigated the integrity of the visual system in *dSap-r* flies. Electron micrographs revealed an abundance of stored material in photoreceptor neurons of the fly retina (Fig. 6A), similar in morphology to that found in the antennal lobe neurons (Fig. 4C). High magnification images showed a variable phenotype in the rhabdomeres, the light responsive component of the eye. Most rhabdomeres showed massive accumulation of electron dense material yet some were found to be structurally intact (Fig. 6A).

To determine whether the photoreceptor neurons and their underlying optic lobe synapses were functionally intact, we measured the ability of the fly eye to respond to light using the electroretinogram (ERG). The ERG is a classic method for investigating photoreceptor and lamina neuron function by measuring the summed potential difference on the surface of the fly eye in response to light pulses (Coombe, 1986; Heisenberg, 1971). Different components of the ERG trace represent the net influence of different parts of the visual system, t: the initial decline in potential reflects the depolarisation of the photoreceptor neurons; the on- and off-transients are a result of synaptic transmission with the L1 and L2 lamina neurons; and the recovery phase denotes the feedback from the optic lobe to the photoreceptor neurons required for efficient repolarisation of the photoreceptors (34-37). Therefore,

the integrity of the different components of visual transduction can be assessed using this simple approach.

ERG recordings in 5-day-old *dSap-r*^{C27}/Df mutants were not significantly different from controls in all components measured (Fig. 6B & C). However, 22-day-old *dSap-r*^{C27}/Df mutants showed a severe deterioration of all components of the ERG compared to controls. The *dSap-r*^{C27}*/Df* mutant ERG potential deteriorated to 46% of its 5-day value, whereas the *dSap-r*^{C27}/+ control ERG potential only decreased to 77% of its 5-day value. This severe deterioration of the ERG amplitude in *dSap-r*^{C27}*/Df* mutants was also matched by a 5-fold increase in recovery time after termination of the light pulse. This suggests that neuronal function in both the retina and underlying optic lobe is severely compromised in *dSap-r* mutants.

Calcium homeostasis is defective in *dSap-r* mutants

Calcium homeostasis defects have been highlighted as one aspect of cellular pathology implicated in the sphinoglipidoses (Ginzburg et al., 2004; Jeyakumar et al., 2005; Lloyd-Evans et al., 2008). For example, in NPC1 cells lysosomal calcium levels have been shown to be abnormally low, and by increasing cytosolic calcium levels NPC pathology in both NPC1 cells and mouse models can be substantially rescued (Lloyd-Evans et al., 2008). Calcium homeostasis defects have also been implicated in other sphingolipidoses (Gaucher's, Sandhoff and GM_1-gangliosidosis)~~:~~; however, in these disorders an increase, rather than a decrease, in cytosolic calcium levels was found to be pathological ~~in these cases~~ (Lloyd-Evans et al., 2003a; Lloyd-Evans et al., 2003b; Pelled et al., 2003; Pelled et al., 2005). This suggests that both abnormally low or abnormally high levels of calcium might be implicated in Sphingolipidoses. Furthermore, calcium homeostasis defects have been mechanistically linked to an imbalance in sphingolipid levels in a fly model of retinal degeneration (Yonamine et al., 2011). Based on our findings of an im~~mis~~balance of sphingolipids prior to severe signs of neurodegeneration in the *dSap-r* mutants, we hypothesised that calcium levels may also be altered.

To investigate calcium misregulation and its impact on~~if the~~ *dSap-r* ~~sphingolipidosis model~~neurodegeneration ~~showed a calcium homeostasis defects~~, we used a similar approach to Yonamine *et al.* (2011) and manipulated calcium levels in the fly eye. ~~measured ERGs in *dSap-r* mutants~~ We overexpress~~ed~~~~ing~~ the plasma membrane calcium exchanger (CalX) in the fly eye using the *NINAE* (Rhodopsin 1) promoter and measured its effect on retinal function using ERGs. CalX transports calcium ions out of the neuron in exchange for sodium ions (Wang et al., 2005). Therefore, if *dSap-r* mutants have a reduced cytosolic calcium level, CalX expression should exacerbate the degeneration and function of the photoreceptors. In contrast,~~;~~ ~~however,~~ the ERG ~~would~~ should be substantially rescued if *dSap-r* mutation causes an increased cytosolic calcium level.

Overexpression of CalX in an otherwise wild type fly resulted in a modest degeneration of the ERG to 81% of its 5-day level (Fig. 6D & E). When CalX was expressed in a *dSap-r*^{C27}/Df mutant background, there was no effect on the 5-day-old *dSap-r*^{C27}/Df mutant ERG. However, as the flies aged, CalX expression induced a decrease in *dSap-r*^{C27}/Df mutant vision to only 9% of its 5-day-old level; this is in contrast to the deterioration of the *dSap-r*^{C27}/Df mutant ERG to 64% of its 5-day-old level, and therefore suggests that the *dSap-r* mutation may cause an abnormally reduced cytosolic calcium level.

Discussion

To further our understanding of the pathology related to saposin deficiency ~~disease~~, we generated a *Drosophila* model. The *Drosophila* prosaposin homologue *dSap-r* was revealed to contain eight saposin-like domains, which all contained the six-cysteine primary sequence common to all saposins (this investigation, (Hazkani-Covo et al., 2002)). We showed that most of the dSap peptides contain a predicted glycosylation site, a feature critical for saposin folding and function (Hiraiwa et al., 1993b). The sequence similarities between the mammalian and *Drosophila* saposins suggested that we had identified the correct ortholog.

To further characterise dSap-r, we investigated its expression pattern using GFP reporters. Both membrane and nuclear GFP reporters confirmed the expression of *dSap-r* in glia, as reported by (Freeman et al., 2003). Although mammalian saposins are expressed in neurons, o~~O~~ur findings ~~also~~ suggested that , ~~unlike in mammals,~~ *dSap-r* is either not expressed in neurons or is expressed at ~~low/undetectable levels~~a level below the threshold of our reporter. Transcriptomic data from FACS isolated neurons, glia and surface glia (blood-brain barrier) (DeSalvo et al., 2014) shows that *dSap-r* is expressed in neurons, glia and surface glia, and may therefore be more ubiquitous than the *dSap-r*^{NP7456} GAL4 enhancer-trap is reporting.

~~Although~~ In addition, mammalian ~~*dSap-r* expression has been shown to occur in glia, this does not discount the presence of dSap-r protein in neurons. Mammalian~~ prosaposin is abundant in secretory fluids, including cerebrospinal fluid, seminal fluid, milk, bile and pancreatic fluid (Hineno et al., 1991; Hiraiwa et al., 1993a; Kondoh et al., 1991; Patton et al., 1997); in fact prosaposin is one of the main secretory products of Sertoli cells in the male reproductive system (Sylvester et al., 1989). Therefore, ~~we propose~~it is quite possible that *Drosophila* glia ~~may~~ provide dSap-r to neurons by glial secretion and neuronal uptake. This notion is ~~supported~~ consistent with~~by~~ our findings that *dSap-r* mutant longevity can be substantially rescued by expressing *dSap-r* directly in neurons, which suggests a neuronal requirement for dSap-r. ~~This is further supported by our TEM analyses showing more severe lysosomal storage and consequential increase in cell size of the neurons compared to the glia.~~ This potential non-autonomous function of dSap-r has important implications for ~~potential~~ future therapeutic strategies as it suggests that a source of prosaposin secreting cells could provide a successful intervention for these conditions.

This investigation also revealed high *dSap-r* expression in the male and female reproductive organs, the digestive system, *Drosophila* renal system (Malpighian tubules), and the *Drosophila* liver equivalent (the fat bodies). Mammalian prosaposin has a role in spermiogenesis and improving fertility

(Amann et al., 1999; Hammerstedt, 1997; Morales et al., 2000; Sun et al., 2007), and is also relatively abundant in subsets of cells of the small intestine, kidney and liver (Sun et al., 1994). Therefore, in addition to having a conserved primary sequence, dSap-r also has a conserved tissue expression suggesting a conserved function.

After confirming the identity of the *Drosophila* prosaposin orthologue and its expression pattern, we generated a *dSap-r* loss-of-function model and assessed its pathology. Ultrastructural analysis revealed extensive storage in the *dSap-r* mutant nervous system (MLBs, enlarged MVBs and lipid droplets), characteristic of LSD pathology. Lysosomal storage was also confirmed by western blotting, which showed progressive accumulation of two lysosomal markers (Arl8 and Cathepsin-L) in the *dSap-r* mutants, and mass spectrometry revealed early accumulation and imbalance of sphingolipid intermediates in *dSap-r* mutants.

The *dSap-r*$^{C27/Df}$ mutants were the most severe mutants in all assays tested. They also showed the most severe imbalance of sphingosine~~: and~~ ceramide, whilst having similar levels of sphingosine and lower levels of ceramide than the other mutant allelic combinations. This therefore supports previous findings that the ratio of sphingolipids is more important than the total levels of individual sphingolipids when considering the effect on pathology (Fewou et al., 2005; Levade et al., 1995; Matsuda et al., 2004; Sun et al., 2008; Sun et al., 2007).

In prosaposin and individual saposin deficiency mouse models, the stored material was described as very heterogeneous with electron-dense and electron-lucent inclusions, MLBs and MVBs (Matsuda et al., 2004; Matsuda et al., 2001; Oya et al., 1998; Sun et al., 2010a; Sun et al., 2010b; Sun et al., 2008; Sun et al., 2007). This phenotype is strikingly similar to the ultrastructural pathology of *dSap-r* mutants.

Like other *Drosophila* LSD models, *dSap-r* mutants die prematurely, with 50% death within 18 days; this equates to a 41-49% reduction in longevity, which is

comparable to most *Drosophila* LSD models (40-55% reduction) (Hickey et al., 2006; Huang et al., 2007; Min and Benzer, 1997; Nakano et al., 2001; Phillips et al., 2008). The *dSap-r* mutants also showed an age-dependent deterioration of spontaneous and evoked locomotion, which correlated with the progressive nature of vacuolarisation in the sensory regions of the *dSap-r* mutant nervous system. This may suggest that locomotion deterioration is primarily a result of failed perception of sensory cues rather than motor neuron or muscle degeneration. This notion is supported by a less severe deterioration in *dSap-r* mutant jump performance using an assay that bypasses sensory neuron input (data not shown). A similar degeneration in sensory function is observed in both *Drosophila* and mouse models of NPC1 (Claudepierre et al., 2010; Palladino et al., 2015; Phillips et al., 2008; Yan et al., 2014), and recently recognised in NPC1 patients (Zafeiriou et al., 2003). These results suggest a particular sensitivity of sensory neurons to disruptions in sphingolipid metabolism. This is also supported by the severe sensory degeneration observed in the sphingolipid synthesis disorder Hereditary Sensory and Autonomic Neuropathy Type 1 (HSAN1) (Dawkins et al., 2001). HSAN1 is caused by mutations in the first enzyme of the sphingolipid synthesis pathway: serine-palmitoyl transferase (SPT). Although HSAN1 is a sphingolipid synthesis disorder and saposin deficiency is a disorder of sphingolipid degradation, the sensory degeneration in both of these disorders reflects a common cellular pathology: a defect in sphingolipid homeostasis. Therefore, sensory degeneration may result from an absence of sphingolipids, an abnormal accumulation of sphingolipids, an imbalance of sphingolipids, or a combination of all three.

Although retinal degeneration and storage has been reported in other *Drosophila* models of LSDs (Dermaut et al., 2005; Myllykangas et al., 2005; Phillips et al., 2008; Tuxworth et al., 2009), the pathological mechanism remains unclear. In several mammalian sphingolipidoses models, recent reports have revealed calcium homeostasis defects. Therefore, a calcium exchanger was overexpressed in the fly eye of *dSap-r* mutants to determine whether altering cytosolic calcium levels had any effect on *dSap-r* mutant retinal function. Aging of *dSap-r*$^{C27/Df}$ mutants caused a 36% reduction in

retinal function; a similar but less severe (19%, n.s.) deterioration was also seen after expression of CalX in aged wild type flies. Overexpression of CalX in a *dSap-r* mutant background caused a severe (92%) deterioration of retinal function, leaving the 22-day-old flies almost completely unresponsive to light. This significant genetic interaction suggests that calcium regulation ~~is~~ may be compromised in *dSap-r* mutant photoreceptors, leading to neurodegeneration and perturbed sensory function. Further work is required to determine the severity of the calcium homeostasis defect in *dSap-r* mutants, including its temporal and spatial (neurons vs glia) involvement.

The *Drosophila* NPC1 model revealed degeneration of the visual system and concomitant deterioration of the ERG that resembles that of the *dSap-r* mutant model (Phillips et al., 2008). Although classically characterised as a cholesterol-storage disorder, mammalian NPC pathology has more recently been linked to sphingolipid storage (Lloyd-Evans et al., 2008), specifically ~~a~~ sphingosine storage leading to a deficit in lysosomal calcium regulation (Lloyd-Evans et al., 2008)~~; therefore, calcium homeostasis may also be dysfunctional in the NPC1 *Drosophila* model.~~ In support of this, in cell culture, NPC1 cells contained approximately 65% less lysosomal calcium compared to control cells. It was shown that the sphingolipid intermediate sphingosine was responsible for this calcium homeostasis defect (Lloyd-Evans et al., 2008), directly linking calcium homeostasis defects to the accumulation of sphingolipids in the sphingolipidoses.

Our sphingolipid analyses showed that sphingosine levels were significantly increased in all *dSap-r* mutant brains. Like in NPC1 cells, this may cause a decrease in lysosomal calcium in *dSap-r* mutants, which was further exacerbated by overexpression of CalX. Further evidence of a link between sphingolipid metabolism and calcium homeostasis was also provided by Yonamine *et al.* (2011), who revealed that retinal degeneration caused by imbalances in sphingolipid metabolites was suppressed by mutations in the *Drosophila CalX*. Similar to Yonamine *et al.*, (2011) w~~W~~e have also shown an imbalance in the ratio between two sphingolipid intermediates in *dSap-r*

mutant brains, providing further support of calcium homeostasis defects being a likely cause of *dSap-r* mutant pathology.

In conclusion, we suggest that ~~in *dSap-r* mutants an~~ early accumulation of sphingosine, or the imbalance of the sphingosine:ceramide ratio, may lead~~s~~ to a decrease in lysosomal calcium and ~~. This calcium deficiency causes~~ degeneration of sensory neurons in ~~the~~ *dSap-r* mutants, which leads ~~ing~~ to physiological deterioration. Therapeutic interventions to increase cytosolic calcium levels in saposin-deficient patients may ~~therefore~~ provide a successful route for ameliorating these disorders.

Funding:

This work was funded by a Quota studentship from the BBSRC [to S.J.H] and a Medical Research Council grant [G0400580 to S.T.S]. Work in the D.S laboratory was supported by a Senior Fellowship of the Wellcome Trust/DBT India Alliance, and the NCBS-Merck & Co International Investigator Award [D.S].

Acknowledgements: For fly stocks and reagents we would like to thank Andreas Prokop, Debbie Smith, Dani Ungar, Roger Hardie, The Bloomington and Kyoto *Drosophila* stock centres and the Developmental Studies Hybridoma Bank, Iowa. The anti-repo, anti-elav and anti-tubulin monoclonal antibodies, developed by Corey Goodman, Gerald M. Rubin and Michael Klymkowsky, were obtained from the DSHB, created by the NICHD of the NIH and maintained at the University of Iowa, Department of Biology, Iowa, IA 52242. We would like to thank Gareth Evans for invaluable help with densitometry and experimental guidance. For technical advice we are indebted to Meg Stark, Karen Hodgkinson, Graeme Park and Paul Pryor.

Conflict of interest statement: none declared

References

Amann, R. P., et al., 1999. Exposure of human, boar, or bull sperm to a synthetic peptide increases binding to an egg-membrane substrate. J Androl. 20**,** 34-41.

Azuma, N., et al., 1994. Stimulation of acid ceramidase activity by saposin D. Arch Biochem Biophys. 311**,** 354-7.

Berent, S. L., Radin, N. S., 1981. Mechanism of activation of glucocerebrosidase by co-beta-glucosidase (glucosidase activator protein). Biochim Biophys Acta. 664**,** 572-82.

Christomanou, H., et al., 1986. Immunochemical characterization of two activator proteins stimulating enzymic sphingomyelin degradation in vitro. Absence of one of them in a human Gaucher disease variant. Biol Chem Hoppe Seyler. 367**,** 879-90.

Claudepierre, T., et al., 2010. Lack of Niemann-Pick type C1 induces age-related degeneration in the mouse retina. Mol Cell Neurosci. 43**,** 164-76.

Coombe, P. E., 1986. The large monopolar cells L1 and L2 are responsible for the ERG transients in Drosophila. J. Comp. Physiol. 159**,** 655-666.

Dawkins, J. L., et al., 2001. Mutations in SPTLC1, encoding serine palmitoyltransferase, long chain base subunit-1, cause hereditary sensory neuropathy type I. Nat Genet. 27**,** 309-12.

Dermaut, B., et al., 2005. Aberrant lysosomal carbohydrate storage accompanies endocytic defects and neurodegeneration in Drosophila benchwarmer. J Cell Biol. 170**,** 127-39.

DeSalvo, M. K., et al., 2014. The Drosophila surface glia transcriptome: evolutionary conserved blood-brain barrier processes. Front Neurosci. 8**,** 346.

Elleder, M., et al., 1984. Niemann-Pick disease type C with enhanced glycolipid storage. Report on further case of so-called lactosylceramidosis. Virchows Arch A Pathol Anat Histopathol. 402**,** 307-17.

Erickson, A. H., 1989. Biosynthesis of lysosomal endopeptidases. J Cell Biochem. 40**,** 31-41.

Fewou, S. N., et al., 2005. Reversal of non-hydroxy:alpha-hydroxy galactosylceramide ratio and unstable myelin in transgenic mice overexpressing UDP-galactose:ceramide galactosyltransferase. J Neurochem. 94**,** 469-81.

Fluegel, M. L., et al., 2006. Mutations of a Drosophila NPC1 gene confer sterol and ecdysone metabolic defects. Genetics. 172**,** 185-96.

Freeman, M. R., et al., 2003. Unwrapping glial biology: Gcm target genes regulating glial development, diversification, and function. Neuron. 38**,** 567-80.

Fujita, N., et al., 1996. Targeted disruption of the mouse sphingolipid activator protein gene: a complex phenotype, including severe leukodystrophy and wide-spread storage of multiple sphingolipids. Hum Mol Genet. 5**,** 711-25.

Furst, W., et al., 1988. The precursor of sulfatide activator protein is processed to three different proteins. Biol Chem Hoppe Seyler. 369**,** 317-28.

Ginzburg, L., et al., 2004. The pathogenesis of glycosphingolipid storage disorders. Semin Cell Dev Biol. 15**,** 417-31.

Hammerstedt, R. H., 1997. A method and use of polypeptide in sperm-egg binding to enhance or decrease fertility. International Patent Publication Number W)/97/25620 Geneva: World International Property Organization. 1-42.

Harzer, K., et al., 1989. Sphingolipid activator protein deficiency in a 16-week-old atypical Gaucher disease patient and his fetal sibling: biochemical signs of combined sphingolipidoses. Eur J Pediatr. 149**,** 31-9.
Hazkani-Covo, E., et al., 2002. The evolutionary history of prosaposin: two successive tandem-duplication events gave rise to the four saposin domains in vertebrates. J Mol Evol. 54**,** 30-4.
Heisenberg, M., 1971. Separation of receptor and lamina potentials in the electroretinogram of normal and mutant Drosophila. J Exp Biol. 55**,** 85-100.
Herzog, R., et al., 2011. A novel informatics concept for high-throughput shotgun lipidomics based on the molecular fragmentation query language. Genome Biol. 12**,** R8.
Hickey, A. J., et al., 2006. Palmitoyl-protein thioesterase 1 deficiency in Drosophila melanogaster causes accumulation of abnormal storage material and reduced life span. Genetics. 172**,** 2379-90.
Hindle, S., et al., 2013. Dopaminergic expression of the Parkinsonian gene LRRK2-G2019S leads to non-autonomous visual neurodegeneration, accelerated by increased neural demands for energy. Hum Mol Genet. 22**,** 2129-40.
Hineno, T., et al., 1991. Secretion of sphingolipid hydrolase activator precursor, prosaposin. Biochem Biophys Res Commun. 176**,** 668-74.
Hiraiwa, M., et al., 1997. Lysosomal proteolysis of prosaposin, the precursor of saposins (sphingolipid activator proteins): its mechanism and inhibition by ganglioside. Arch Biochem Biophys. 341**,** 17-24.
Hiraiwa, M., et al., 1993a. Isolation, characterization, and proteolysis of human prosaposin, the precursor of saposins (sphingolipid activator proteins). Arch Biochem Biophys. 304**,** 110-6.
Hiraiwa, M., et al., 1993b. The effect of carbohydrate removal on stability and activity of saposin B. Arch Biochem Biophys. 303**,** 326-31.
Hofmann, I., Munro, S., 2006. An N-terminally acetylated Arf-like GTPase is localised to lysosomes and affects their motility. J Cell Sci. 119**,** 1494-503.
Huang, X., et al., 2005. A Drosophila model of the Niemann-Pick type C lysosome storage disease: dnpc1a is required for molting and sterol homeostasis. Development. 132**,** 5115-24.
Huang, X., et al., 2007. Drosophila Niemann-Pick type C-2 genes control sterol homeostasis and steroid biosynthesis: a model of human neurodegenerative disease. Development. 134**,** 3733-42.
Hulkova, H., et al., 2001. A novel mutation in the coding region of the prosaposin gene leads to a complete deficiency of prosaposin and saposins, and is associated with a complex sphingolipidosis dominated by lactosylceramide accumulation. Hum Mol Genet. 10**,** 927-40.
Jardim, L. B., et al., 2010. Clinical aspects of neuropathic lysosomal storage disorders. J Inherit Metab Dis. 33**,** 315-29.
Jeyakumar, M., et al., 2005. Storage solutions: treating lysosomal disorders of the brain. Nat Rev Neurosci. 6**,** 713-25.
Kondoh, K., et al., 1991. Isolation and characterization of prosaposin from human milk. Biochem Biophys Res Commun. 181**,** 286-92.
Levade, T., et al., 1995. Neurodegenerative course in ceramidase deficiency (Farber disease) correlates with the residual lysosomal ceramide turnover in cultured living patient cells. J Neurol Sci. 134**,** 108-14.
Lloyd-Evans, E., et al., 2008. Niemann-Pick disease type C1 is a sphingosine storage disease that causes deregulation of lysosomal calcium. Nat Med. 14**,** 1247-55.

Lloyd-Evans, E., et al., 2003a. Glucosylceramide and glucosylsphingosine modulate calcium mobilization from brain microsomes via different mechanisms. J Biol Chem. 278**,** 23594-9.
Lloyd-Evans, E., et al., 2003b. Lyso-glycosphingolipids mobilize calcium from brain microsomes via multiple mechanisms. Biochem J. 375**,** 561-5.
Matsuda, J., et al., 2004. Mutation in saposin D domain of sphingolipid activator protein gene causes urinary system defects and cerebellar Purkinje cell degeneration with accumulation of hydroxy fatty acid-containing ceramide in mouse. Hum Mol Genet. 13**,** 2709-23.
Matsuda, J., et al., 2001. A mutation in the saposin A domain of the sphingolipid activator protein (prosaposin) gene results in a late-onset, chronic form of globoid cell leukodystrophy in the mouse. Hum Mol Genet. 10**,** 1191-9.
Matyash, V., et al., 2008. Lipid extraction by methyl-tert-butyl ether for high-throughput lipidomics. J Lipid Res. 49**,** 1137-46.
Min, K. T., Benzer, S., 1997. Spongecake and eggroll: two hereditary diseases in Drosophila resemble patterns of human brain degeneration. Curr Biol. 7**,** 885-8.
Morales, C. R., et al., 2000. Targeted disruption of the mouse prosaposin gene affects the development of the prostate gland and other male reproductive organs. J Androl. 21**,** 765-75.
Morimoto, S., et al., 1989. Saposin A: second cerebrosidase activator protein. Proc Natl Acad Sci U S A. 86**,** 3389-93.
Myllykangas, L., et al., 2005. Cathepsin D-deficient Drosophila recapitulate the key features of neuronal ceroid lipofuscinoses. Neurobiol Dis. 19**,** 194-9.
Nakano, T., et al., 1989. Structure of full-length cDNA coding for sulfatide activator, a Co-beta-glucosidase and two other homologous proteins: two alternate forms of the sulfatide activator. J Biochem. 105**,** 152-4.
Nakano, Y., et al., 2001. Mutations in the novel membrane protein spinster interfere with programmed cell death and cause neural degeneration in Drosophila melanogaster. Mol Cell Biol. 21**,** 3775-88.
O'Brien, J. S., Kishimoto, Y., 1991. Saposin proteins: structure, function, and role in human lysosomal storage disorders. FASEB J. 5**,** 301-8.
O'Brien, J. S., et al., 1988. Coding of two sphingolipid activator proteins (SAP-1 and SAP-2) by same genetic locus. Science. 241**,** 1098-101.
Oya, Y., et al., 1998. Pathological study of mice with total deficiency of sphingolipid activator proteins (SAP knockout mice). Acta Neuropathol. 96**,** 29-40.
Palladino, G., et al., 2015. Visual evoked potentials of Niemann-Pick type C1 mice reveal an impairment of the visual pathway that is rescued by 2-hydroxypropyl-ss-cyclodextrin. Orphanet J Rare Dis. 10**,** 133.
Patton, S., et al., 1997. Prosaposin, a neurotrophic factor: presence and properties in milk. J Dairy Sci. 80**,** 264-72.
Pelled, D., et al., 2003. Inhibition of calcium uptake via the sarco/endoplasmic reticulum Ca2+-ATPase in a mouse model of Sandhoff disease and prevention by treatment with N-butyldeoxynojirimycin. J Biol Chem. 278**,** 29496-501.
Pelled, D., et al., 2005. Enhanced calcium release in the acute neuronopathic form of Gaucher disease. Neurobiol Dis. 18**,** 83-8.
Phillips, S. E., et al., 2008. Neuronal loss of Drosophila NPC1a causes cholesterol aggregation and age-progressive neurodegeneration. J Neurosci. 28**,** 6569-82.
Schwudke, D., et al., 2011. Shotgun lipidomics on high resolution mass spectrometers. Cold Spring Harb Perspect Biol. 3**,** a004614.

Spiegel, R., et al., 2005. A mutation in the saposin A coding region of the prosaposin gene in an infant presenting as Krabbe disease: first report of saposin A deficiency in humans. Mol Genet Metab. 84**,** 160-6.
Spurr, A. R., 1969. A low-viscosity epoxy resin embedding medium for electron microscopy. J Ultrastruct Res. 26**,** 31-43.
Sun, Y., et al., 2010a. Neuronopathic Gaucher disease in the mouse: viable combined selective saposin C deficiency and mutant glucocerebrosidase (V394L) mice with glucosylsphingosine and glucosylceramide accumulation and progressive neurological deficits. Hum Mol Genet. 19**,** 1088-97.
Sun, Y., et al., 2010b. Specific saposin C deficiency: CNS impairment and acid beta-glucosidase effects in the mouse. Hum Mol Genet. 19**,** 634-47.
Sun, Y., et al., 1994. Developmental and tissue-specific expression of prosaposin mRNA in murine tissues. Am J Pathol. 145**,** 1390-8.
Sun, Y., et al., 2008. Neurological deficits and glycosphingolipid accumulation in saposin B deficient mice. Hum Mol Genet. 17**,** 2345-56.
Sun, Y., et al., 2007. Combined saposin C and D deficiencies in mice lead to a neuronopathic phenotype, glucosylceramide and alpha-hydroxy ceramide accumulation, and altered prosaposin trafficking. Hum Mol Genet. 16**,** 957-71.
Sylvester, S. R., et al., 1989. Sulfated glycoprotein-1 (saposin precursor) in the reproductive tract of the male rat. Biol Reprod. 41**,** 941-8.
Tuxworth, R. I., et al., 2009. Interactions between the juvenile Batten disease gene, CLN3, and the Notch and JNK signalling pathways. Hum Mol Genet. 18**,** 667-78.
Tylki-Szymanska, A., et al., 2007. Non-neuronopathic Gaucher disease due to saposin C deficiency. Clin Genet. 72**,** 538-42.
Van Den Berghe, L., et al., 2004. Prosaposin gene expression in normal and dystrophic RCS rat retina. Invest Ophthalmol Vis Sci. 45**,** 1297-305.
Vogel, A., et al., 1987. Identity of the activator proteins for the enzymatic hydrolysis of sulfatide, ganglioside GM1, and globotriaosylceramide. Arch Biochem Biophys. 259**,** 627-38.
Wang, T., et al., 2005. Light activation, adaptation, and cell survival functions of the Na+/Ca2+ exchanger CalX. Neuron. 45**,** 367-78.
Yamada, M., et al., 2004. Analysis of recombinant human saposin A expressed by Pichia pastoris. Biochem Biophys Res Commun. 318**,** 588-93.
Yan, X., et al., 2014. Defects in the retina of Niemann-pick type C 1 mutant mice. BMC Neurosci. 15**,** 126.
Yonamine, I., et al., 2011. Sphingosine kinases and their metabolites modulate endolysosomal trafficking in photoreceptors. J Cell Biol. 192**,** 557-67.
Yoneshige, A., et al., 2009. Regional expression of prosaposin in the wild-type and saposin D-deficient mouse brain detected by an anti-mouse prosaposin-specific antibody. Proc Jpn Acad Ser B Phys Biol Sci. 85**,** 422-34.
Yuan, C., et al., 2011. CDase is a pan-ceramidase in Drosophila. Mol Biol Cell. 22**,** 33-43.
Zafeiriou, D. I., et al., 2003. Niemann-Pick type C disease associated with peripheral neuropathy. Pediatr Neurol. 29**,** 242-4.

Figure Legends

Fig. 1. *Drosophila Sap-r* is expressed in glia. A. The *Drosophila prosaposin* homologue *Saposin-related* (*dSap-r*) consists of seven exons and is present on the right arm of the third chromosome (3R) at position 100A7. The *dSap-r* gene contains two potential transcript start sites (ATG), which result in the production of a transcript consisting of the entire coding sequence (*dSap-rRA*, 3451 bp) and an in-frame, truncated version (*dSap-rRB*, 3349 bp) (black lines). The *dSap-r*^{C27} mutant allele was generated by *P*-element mobilisation from the *P*{GawB}NP7456 line and is a 2.5kb deletion. The *dSap-r*^{PBac} mutant allele consists of a 5.971 bp piggyBac transposon insertion into the largest *dSap-r* exon. The deletion in the deficiency line Df(3R)*tll-e* spans cytogenetic bands 100A2 – 100C5, which includes the *dSap-r* gene. B. A Clustal X alignment of the 8 predicted *Drosophila melanogaster* saposins (dSaps) and the 4 *Homo sapiens* saposins (hSaps). Asterisks, conserved cysteine residues; underlining, glycosylation sites in each hSap and possible homologous sites in the dSaps. Blue highlights identical residues; yellow highlights similar residues (80% threshold setting). C. Confocal images of third instar larvae brains expressing mCD8eGFP or eIF4AIIIGFP (n>5) under the control of *dSap-r*^{NP7456} GAL4 and stained with α-repo (glial nuclear marker) or α-elav (pan neuronal marker). Scale bars: 20 μm.

Fig. 2. Reduced longevity ~~and physiological deterioration~~ in *dSap-r* mutants. A & B. Longevity of flies with different *dSap-r* mutant allelic combinations was assessed at 29°C. Rescue of *dSap-r* mutant longevity was performed by expressing *dSap-r* cDNA in the neurons (A) or glia (B) of *dSap-r* mutants using the 1407- and repo-GAL4 drivers. Neuronal or glial expression of *dSap-r* in a wild type background was performed as a transgene control. Longevity was plotted as the percentage of Day 0 flies surviving for each genotype. n > 60 flies for each genotype. C. cDNA from wild type (+/+), *dSap-r*^{PBac}/Df (PBac/Df) mutant and *dSap-r*^{C27}/Df (C27/Df) mutant third instar larvae were amplified using *rp49* control and *dSap-r* primers.

~~D. 5-day-old (white bars) and 22-day-old flies (grey bars) were subjected to climbing assays. The climbing speed of *dSap-r*^{C27} heterozygotes (C27/+), *dSap-r*^{C27}/Df (C27/Df) and *dSap-r*$^{C27/PBac}$ (C27/PBac) mutants are shown. Error bars: ± sem. * p< 0.05, ** p< 0.005 and *** p≤ 0.001.~~

Fig. 3. Progressive neurodegeneration in sensory regions of *dSap-r* mutants. A. Representative images of 1 μm sections through 5-day-old and 22-day-old control (dSap-r$^{C27/}$+) and *dSap-r* mutant (*dSap-r*^{C27}/Df and *dSap-r*$^{C27/PBac}$) heads are shown at

Formatted: Keep with next

Formatted: None, Space Before: 0 pt, After: 0 pt, Don't keep with next

20x magnification (top 2 rows) and 63x magnification (bottom 2 rows, eye (upper row) and antennal lobe (lower row)). Scale bars: 100 μm. B & C. Quantification of vacuole number was performed on 3 serial sections per fly (n≥3 flies). Vacuoles were counted for the visual (B; eye, lamina, medulla and lobula complex) and olfactory (C; antennal lobes) systems at~~in~~ both sides of the brain. Quantification is shown for all controls and *dSap-r* mutants tested. Genotypes tested: +/+ (wild type); Df/+, PBac/+ and C27/+ (*dSap-r* heterozygotes); PBac/Df, C27/Df and C27/PBac (*dSap-r* mutants). Error bars: ± sem. *** p≤ 0.001

Fig. 4. Progressive lysosomal storage in *dSap-r* mutants. A. Western blots showing the abundance of the lysosomal proteins Arl-8 and Cathepsin-L in 5-day-old and 22-day-old wild type (+/+), *dSap-r*^{C27}/Df (C27/Df), *dSap-r*$^{C27/PBac}$ (C27/PBac) and *dSap-r*^{PBac}/Df (PBac/Df) mutants (n=2). Tubulin abundance is show as a loading control. Average band intensities and S.E.M are shown below. ~~-~~B. Confocal micrographs of 22-day-old wild type (+/+) and *dSap-r*^{C27}/Df mutant brains showing Arl-8 localisation and abundance (n>8). Elav staining shows the similar orientation of both wild type and *dSap-r*^{C27}/Df mutant brains. Scale bar: 100 μm. ~~C. Transmission electron micrographs of 22-day-old wild type (+/+) and *dSap-r*^{C27}/Df mutant neuronal cell bodies surrounding the antennal lobes. Multivesicular bodies and multilamellar bodies (arrows) are abundant in *dSap-r*^{C27}/Df mutant neuronal cell bodies. Scale bars: 2 μm (i - v), 100 nm (vi). D & E. Quantification of sphingosine levels (D) and the sphingosine:ceramide ratio in 5-day-old controls and *dSap-r* mutant brains. Genotypes tested: +/+ (wild type); Df/+, PBac/+ and C27/+ (*dSap-r* heterozygotes); PBac/Df, C27/Df and C27/PBac (*dSap-r* mutants). * p<0.05, *** p<0.001 and **** p<0.0001.~~

Fig. 5. Neuronal swelling, degeneration and lipid storage are abundant in *dSap-r* mutant brains A. Transmission electron micrographs showing neuronal cell bodies adjacent to the antennal lobes of 22-day-old wild type (+/+) and *dSap-r*^{C27}/Df mutants (n=3). Each soma has been demarcated in grey and rendered a different pseudocolour. The nuclei are demarcated by dashed lines. T, trachea; V, vacuole; white asterisk, fat body. Scale bar: 2 μm. B & C. Quantification of 22-day-old wild type (+/+) and *dSap-r*^{C27}/Df (C27/Df) mutant soma area (B) and cell:nucleus ratio (C). ** p<0.005. ~~**have grossly enlarged soma size**~~ D. Transmission electron micrographs of 22-day-old wild type (+/+) and *dSap-r*^{C27}/Df mutant neuronal cell bodies surrounding the antennal lobes (n=3). Multivesicular bodies and multilamellar bodies (arrows) are abundant in *dSap-r*^{C27}/Df mutant neuronal cell bodies. Scale bars: 2 μm (i - v), 100 nm (vi). E~~A~~. Transmission electron micrographs showing the integrity of the ommatidia in 22-day-old wild type (+/+) and *dSap-r*^{C27}/Df mutants. Arrowheads mark vacuoles and arrows mark electron lucent material within regions of electron-dense storage. Scale bars: 5 μm (i & iv), 2 μm (ii & v) and 500 nm (iii & vi). F-I. Quantification of sphingosine levels (F), the sphingosine:ceramide ratio (G), the phosphatidylinositol level (H), and Phosphatidylserine (I) in 5-day-old controls and *dSap-r* mutant brains. Genotypes tested: +/+ (wild type); Df/+, PBac/+ and C27/+ (*dSap-r* heterozygotes); PBac/Df, C27/Df and C27/PBac (*dSap-r* mutants). * p<0.05, **p<0.01, ***p<0.000, ****p<0.0001 as determined by ANOVA followed by post-hoc Bonferonni test.

~~A. Transmission electron micrographs showing neuronal cell bodies adjacent to the antennal lobes of 22-day-old wild type (+/+) and *dSap-r*^{C27}/Df mutants. Each soma has been demarcated in grey and rendered a different pseudocolour. The nuclei are demarcated by dashed lines. T, trachea; V, vacuole. Scale bar: 2 μm. B & C.~~

~~Quantification of 22-day-old wild type (+/+) and *dSap-r*^{C27}/Df (C27/Df) soma area (B) and cell:nucleus ratio (C). ** p<0.005.~~ ~~Table depicts the significant changes in levels of major sphingolipids and phospholipids (quantified as picomoles/□g protein) in brains of mutant alleles as compared to +/+ (Canton-S; Control). A minimum of 4 replicates were used for the analyses. Statistically significant changes are indicated by green (increase) and red (decrease). * p<0.01, **p<0.001, ***p<0.0001 as determined by ANOVA followed by post-hoc Bonferonni test.~~

Fig. 6. Calcium homeostasis defects are associated with progressive deterioration of visual function in *dSap-r* mutants. A. 5-day-old (white bars) and 22-day-old flies (grey bars) were subjected to climbing assays (n>20 flies). The climbing speed of *dSap-r*^{C27} heterozygotes (C27/+), *dSap-r*^{C27}/Df (C27/Df) and *dSap-r*$^{C27/PBac}$ (C27/PBac) mutants are shown. Error bars: ± sem. ** p< 0.005 and *** p≤ 0.001. ~~A. Transmission electron micrographs showing the integrity of the ommatidia in 22-day-old wild type (+/+) and *dSap-r*^{C27}/Df mutants. Arrowheads mark vacuoles and arrows mark electron lucent material within regions of electron-dense storage. Scale bars: 5 μm (i & iv), 2 μm (ii & v) and 500 nm (iii & vi).~~ B. Quantification of electroretinogram (ERG) amplitude and recovery rate after a blue light pulse. The recovery rate is the time taken for the potential to reach half way between the off-transient and base-line potentials after termination of the light pulse. C. Representative ERG traces for 5-day-old and 22-day-old control (*dSap-r*^{C27}/+) and *dSap-r*^{C27}/Df -mutant females following a blue light pulse. D. Quantification of ERG amplitude after a blue light pulse in 5-day-old and 22-day-old wild type overexpressing the calcium exchanger CalX in the eye (CalX/+), *dSap-r*^{C27}/Df mutants (C27/Df) and *dSap-r*^{C27}/Df mutants overexpressing CalX in the eye (CalX/+;C27/Df). E. Representative ERG traces for 5-day-old and 22-day-old wild type overexpressing CalX (CalX/+), *dSap-r*^{C27}/Df mutants and *dSap-r*^{C27}/Df mutants expressing CalX (CalX; *dSap-r*^{C27}/Df). N ≥ 7 flies per condition. *** p≤0.001

Formatted: None, Space Before: 0 pt, After: 0 pt, Don't keep with next

Supplemental Fig. 1

***dSap-r* is expressed in visceral organs of *Drosophila*.** Digestive systems (A), male (B) and female (D) reproductive systems and fat bodies (C) are shown from adult controls (+/+) and flies expressing mCD8eGFP under the control of *dSap-r*^{NP7456} GAL4. Organs are stained with the nuclear marker DAPI in (A). MT, Malpighian tubule; Mg, midgut; Hg, hindgut; T, testes; EB, ejaculatory bulb; AG, accessory gland; ED, ejaculatory duct; O, ovary; S, spermatheca. Scale bars: (A) 1000 μm (vii) and 250 μm (viii), (B-D) 500 μm.

Supplemental Fig. 2

Cell enlargement and increased storage in *dSap-r*^{C27}/Df mutant glia. Transmission electron micrographs of glia surrounding the antennal lobe of 22-day old wild type (+/+; A) and *dSap-r*^{C27}/Df mutant (B) brains (n = 3). Electron-dense and

electron-lucent vesicular storage is shown in *dSap-r*^{C27}/Df mutant glia (B). Scale bar: 1 µm. ~~n = 3~~

Supplemental Table 1: Summary of lipidome-wide changes in *dSap-r* mutant brains

Table depicts the significant changes in levels of major sphingolipids and phospholipids (quantified as picomoles/□g protein) in brains of mutant alleles as compared to +/+ (Canton-S; Control). A minimum of 4 replicates were used for the analyses. Statistically significant changes are indicated by green (increase) and red (decrease). * p<0.01, **p<0.001, ***p<0.0001 as determined by ANOVA followed by post hoc Bonferonni test.

picomoles/□g protein		Df/+	C27/+	PBac/+	C27/Df	C27/PBac	PBac/Df
Phospholipids (in order of abundance in fly brain)	PE	-	-	-	-	-	-
	PE-O	-	-	-		-	
	LPE	-	-	-	-	-	-
	PC	-	-	-			-
	PI	-	-	-	-	-	*
	PS						
Sphingolipids	CerPE	-	-	-	-	***	***
	Ceramide	-	-	-	-	***	***
	Sphingosine	-	-	-	***	*	***
	HexCer	-	-	-	-	-	-

PE: Phosphatidylethanolamine

PE-O: Phosphatidylethanolamine Ether

LPE: Lyso-Phosphatidylethanolamine

PC: Phosphatidylcholine

PI: Phosphatidylinositol

PS: Phosphatidylserine

CerPE: Ceramide Phosphorylethalolamine

HexCer: Hexosyl-Ceramide

Supplemental Table 12: Internal Standard (IS) mix used for lipidomics

Formatted: Line spacing: 1.5 lines

LIPID STANDARD	Catalog No.	SOURCE	Amount added to extract (pmol)
CerPE-C12 Sphingosyl PE [d17:1]	110753	Avanti Polar Lipids, USA	7.96
PC [17:0-14:1]	LM-1004		4.43
PE [17:1-14:0]	LM1104		4.29
C17-Cer [d18:1/17:0]	860517P		10.41
PE-OO [40:00]	999985P		7.16
Sphingosine [d17:1]	LM-2000		7.1
PI [17:0-14:1]	LM-1504		3.72
GluCer[d18:1/12:0]	860543P		7.89
PS [17:0-14:1]	LM-11304		2.95

Figure

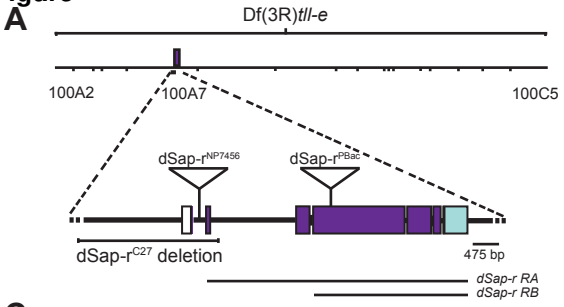

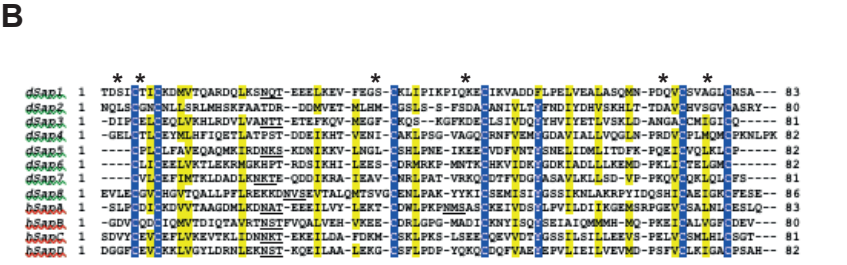

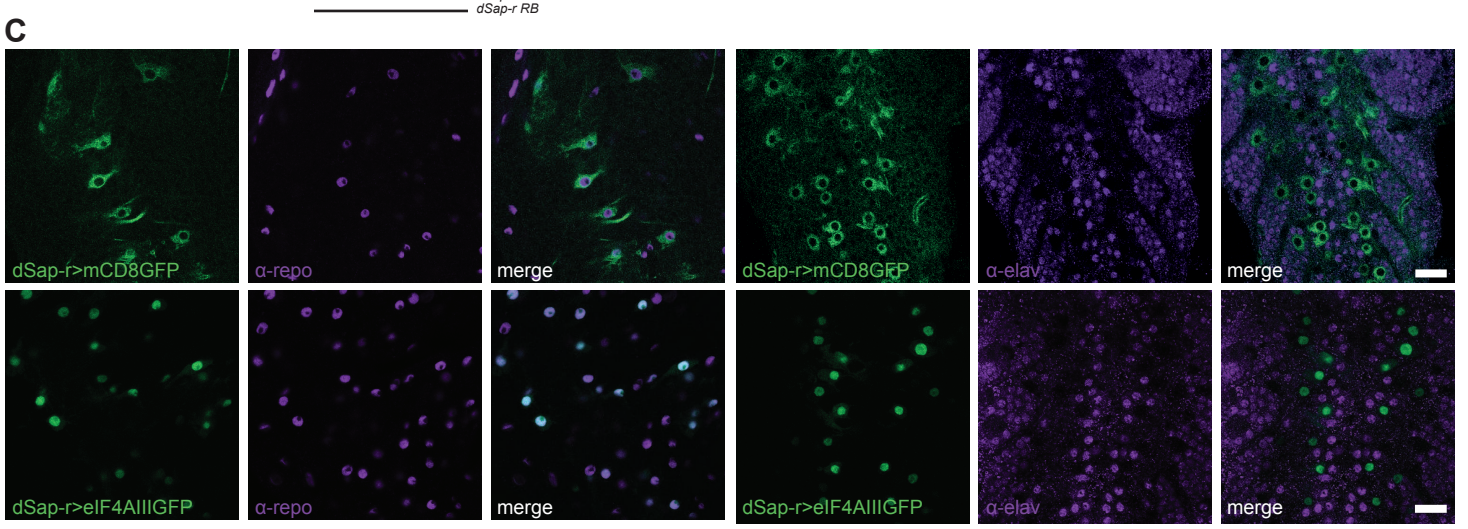

Figure 1

Figure

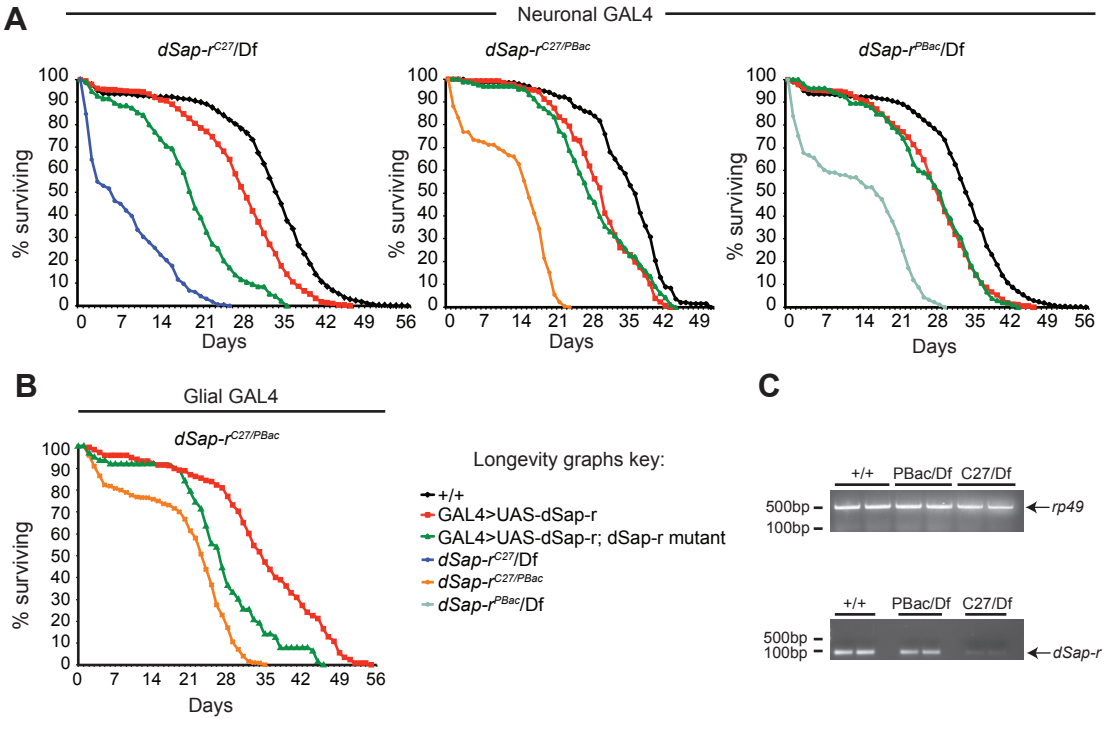

Figure 2

Figure

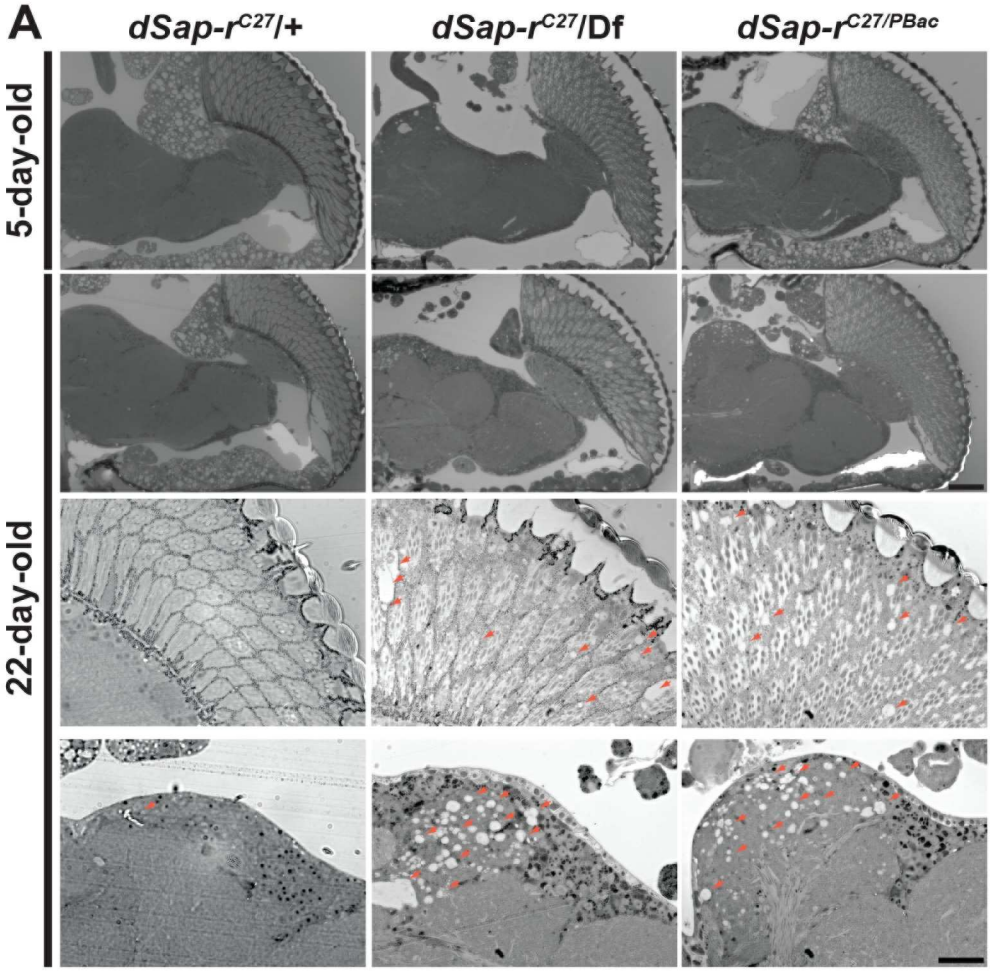

e

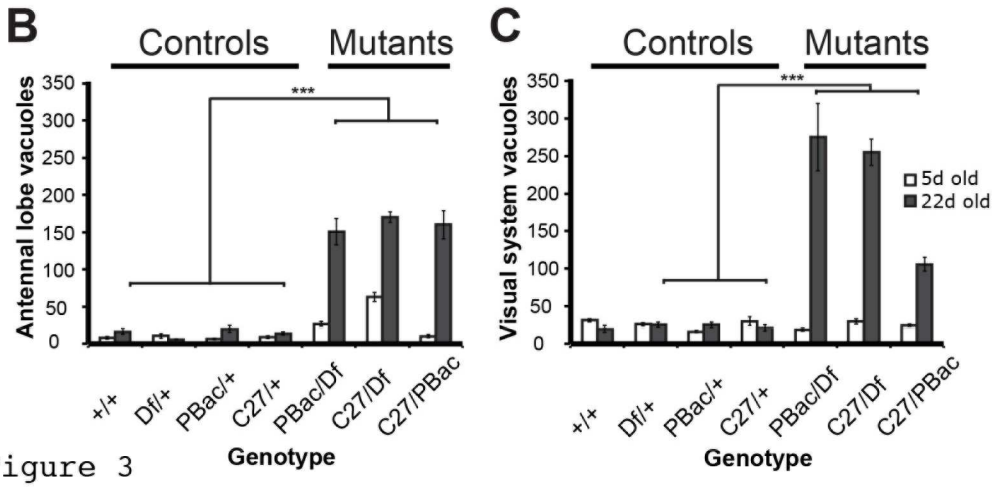

Figure 3

Figure

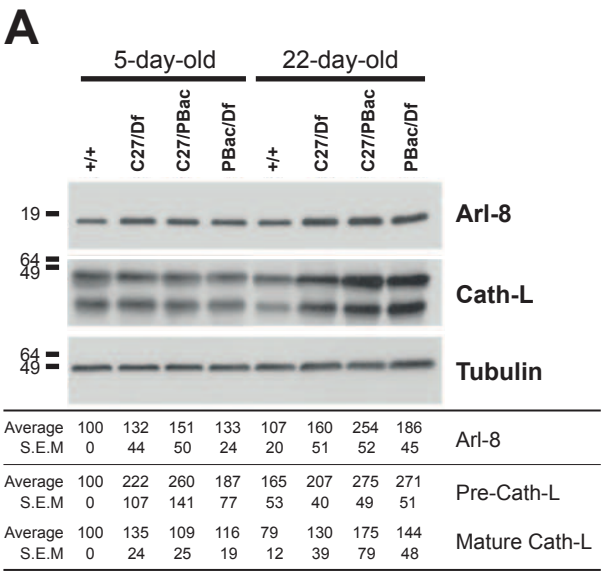

Average	100	132	151	133	107	160	254	186	Arl-8
S.E.M	0	44	50	24	20	51	52	45	
Average	100	222	260	187	165	207	275	271	Pre-Cath-L
S.E.M	0	107	141	77	53	40	49	51	
Average	100	135	109	116	79	130	175	144	Mature Cath-L
S.E.M	0	24	25	19	12	39	79	48	

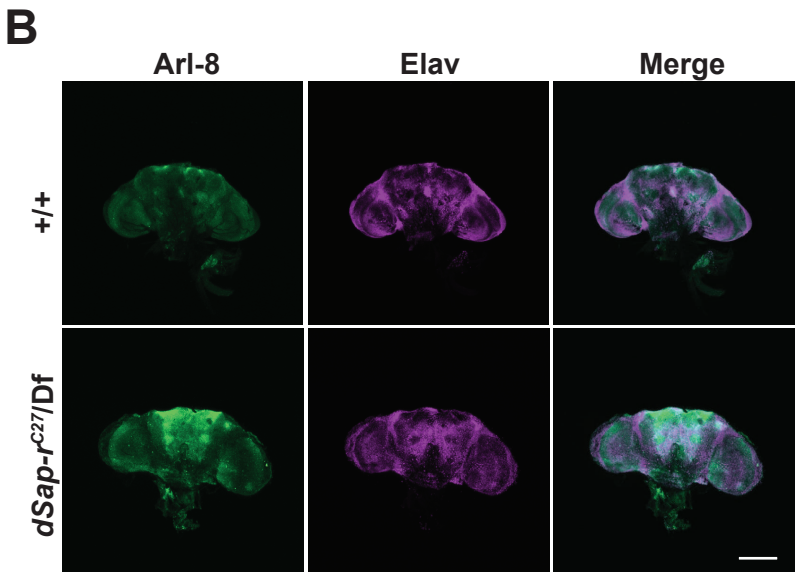

Figure 4

Figure

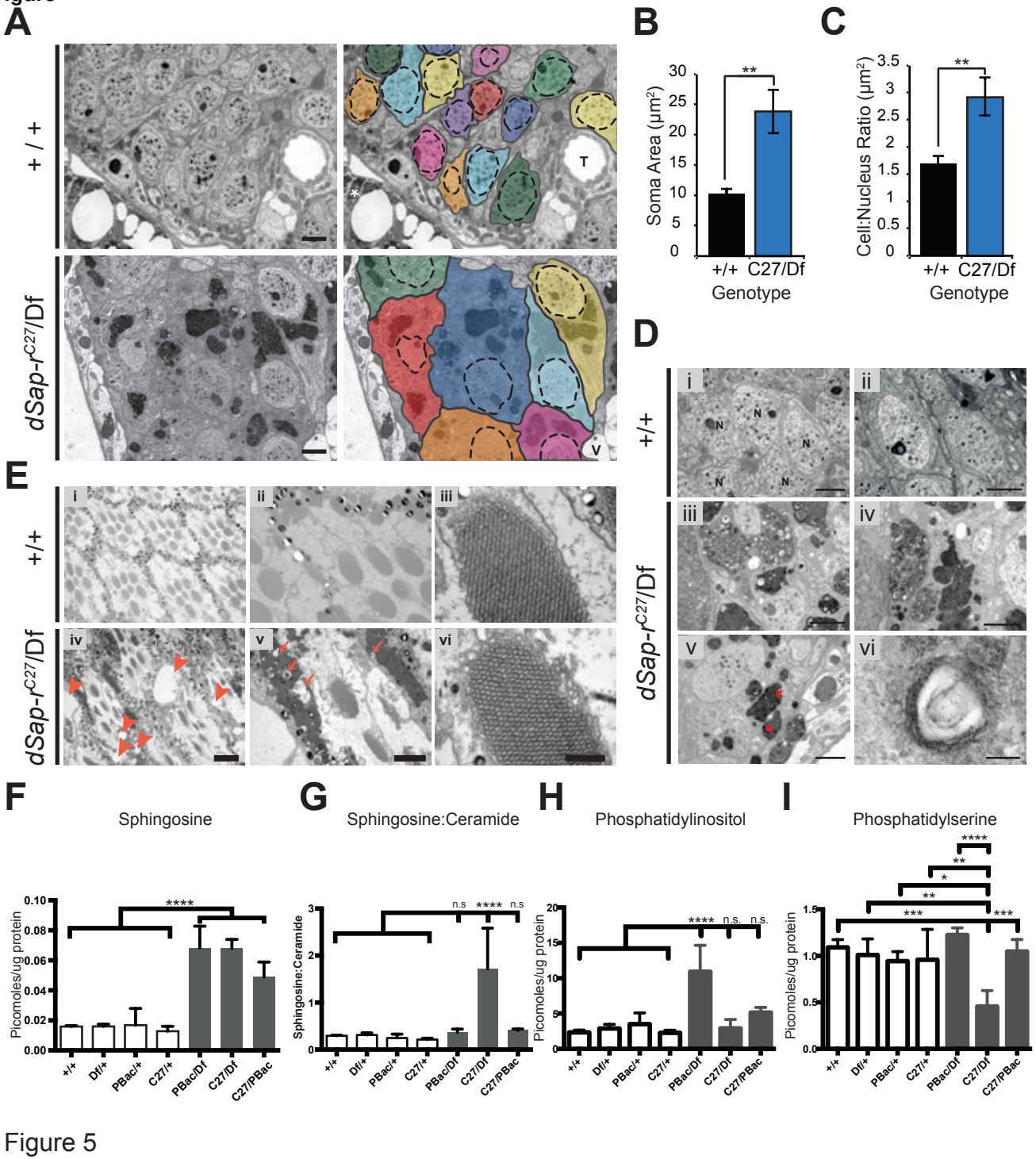

Figure 5

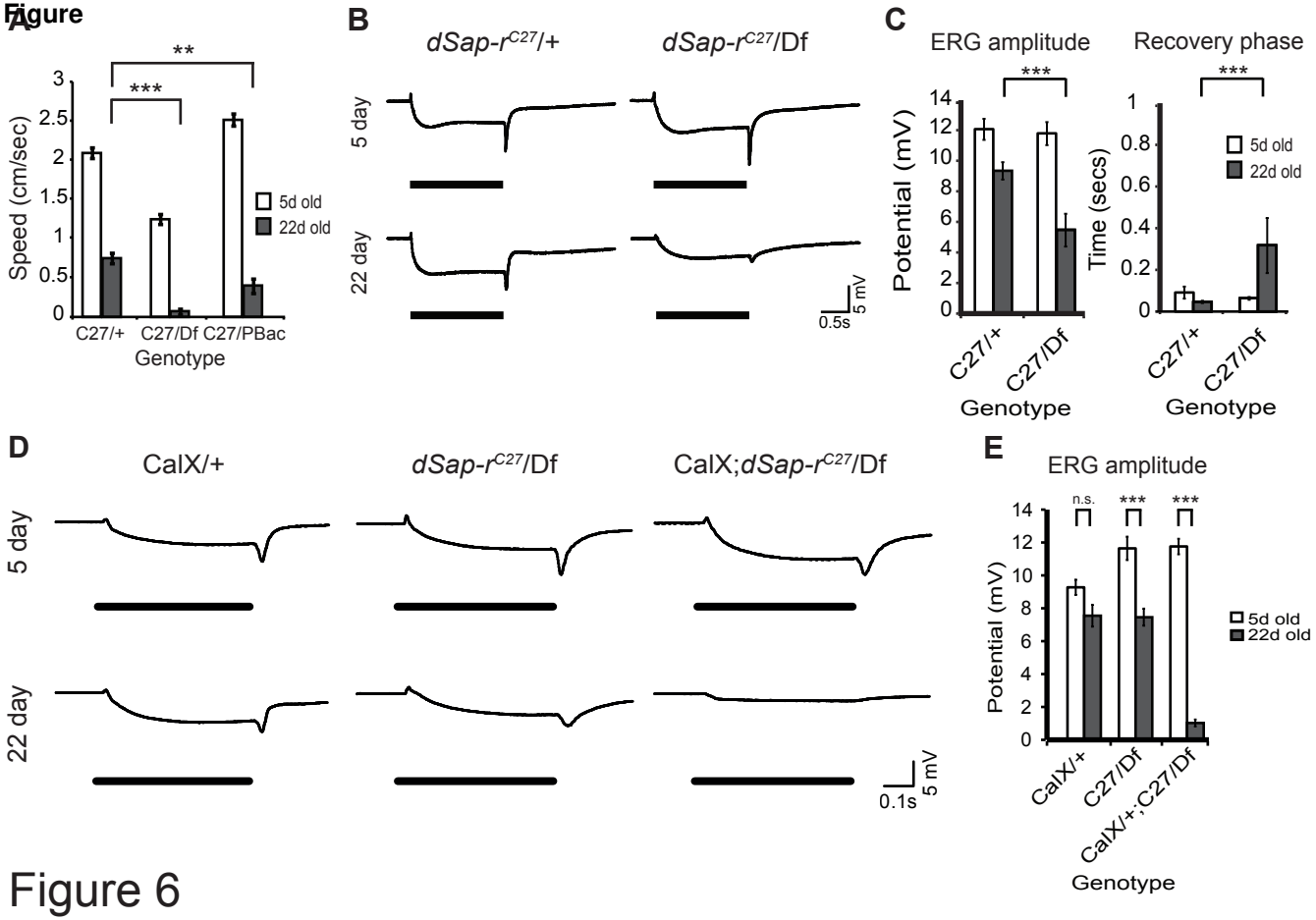
A
Speed (cm/sec)
3
2.5
2
1.5
1
0.5
0
**
***
5d old
22d old
C27/+
C27/Df
C27/PBac
Genotype
B
dSap-r^C27/+
dSap-r^C27/Df
5 day
22 day
0.5s
5 mV
C
ERG amplitude
Recovery phase
***
***
Potential (mV)
Time (secs)
14
12
10
8
6
4
2
0
1
0.8
0.6
0.4
0.2
0
5d old
22d old
C27/+
C27/Df
Genotype
D
CalX/+
dSap-r^C27/Df
CalX;dSap-r^C27/Df
5 day
22 day
0.1s
5 mV
E
ERG amplitude
n.s.
***
***
Potential (mV)
14
12
10
8
6
4
2
0
5d old
22d old
CalX/+
C27/Df
CalX/+;C27/Df
Genotype

Figure 6

Supplementary Material

Click here to download Supplementary Material: Supplemental Fig1.pdf

Supplementary Material

Click here to download Supplementary Material: Supplemental Fig 2.pdf